

3-Tooth Conformal Biofilm FEM

BioFilm3T Pipeline: Mesh → Assembly → ABAQUS → Condition Comparison

Report generated 2026-02-22 (P0 updated 2026-02-22) · IKM Hiwi

Nishioka

2026-02-22

Contents

1 Executive Summary	3
2 Pipeline Overview	4
2.1 Data flow	4
2.2 Unit system	4
2.3 Key files	4
3 Geometry: OpenJaw Teeth	5
4 Mesh Generation Algorithm	5
4.1 Step 1 — STL reading and vertex deduplication	5
4.2 Step 2 — Vertex normals	5
4.3 Step 3 — Offset surface generation	5
4.4 Step 4 — Prism-to-tet split (canonical split)	5
4.5 Mesh statistics	6
5 Material Model	6
5.1 DI-to-stiffness mapping	6
5.2 Effective elastic modulus	6
5.3 Sensitivity of E_{\max} , E_{\min} , and DI transform	7
6 3-Tooth Assembly	8
6.1 Node and element numbering	8
6.2 Approximal (slit) face detection	8
6.3 Tie constraint (slit coupling)	8
7 Boundary Conditions and Loading	9
7.1 Boundary conditions	9
7.2 Loading	9
7.3 Step parameters	9
8 Abaqus Run	10
8.1 Run commands	10
8.2 Run status	10
9 Results	10
9.1 Numerical summary	10
9.2 Figures	11

10 TMCMC → FEM Condition Comparison (P0 / P7)	16
10.1 Motivation	16
10.2 Conditions compared	16
10.3 DI field and material stiffness	17
10.4 Abaqus solve — commensal-static	17
10.5 Posterior ensemble Mises stress	17
10.6 Comparison figures	18
10.7 Late-time condition comparison (P0b)	20
10.8 Geometry scope and limitations	23
11 Known Issues and Lessons Learned	24
12 Next Actions	24
13 Material-model sensitivity (P9)	26
14 BC sensitivity: force vs displacement control (P10)	28
15 Documentation Roadmap	30
A Material Bin Table	30
B ODB Extraction Details	30

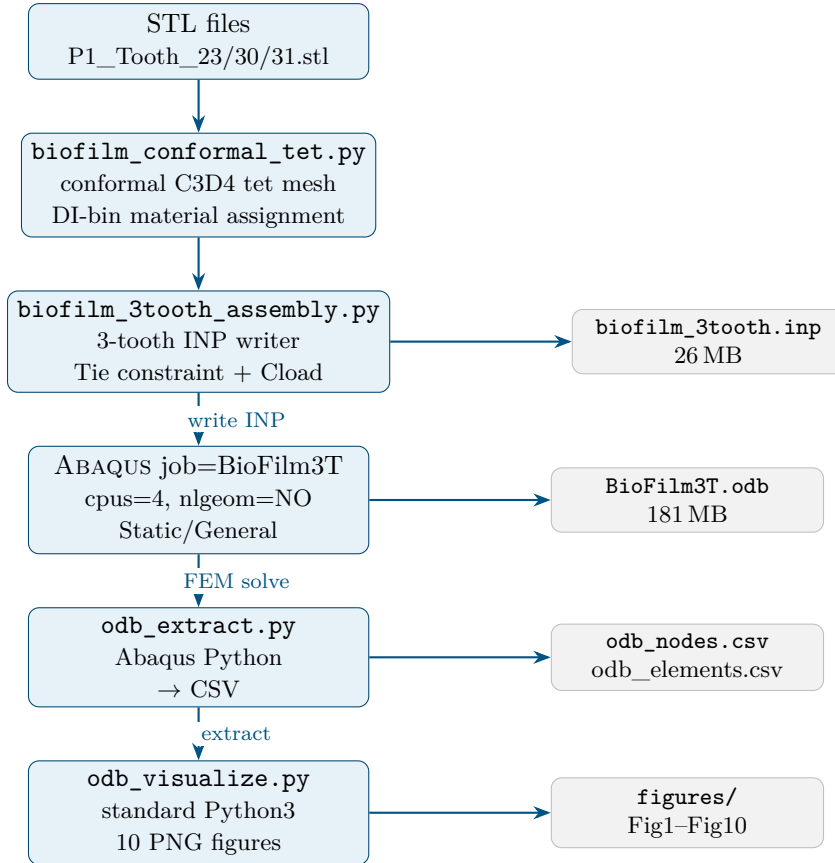
1 Executive Summary

This report documents the complete **BioFilm3T** finite-element pipeline: conformal tetrahedral biofilm meshing of three real human teeth (Patient 1, Teeth T23/T30/T31) from the OpenJaw dataset, assembly into a single ABAQUS/Standard model, computation of von Mises stress and nodal displacement under inward masticatory pressure, and ten-figure visualisation.

Item	Value
Mesh nodes (total)	82 080
C3D4 elements (total)	437 472
Biofilm thickness	0.5 mm
Layer resolution through thickness	8
DI material bins	20 (7 active)
Applied pressure	1 MPa (inward)
Baseline (DH-baseline) run	
MISES median (T23 crown)	0.546 MPa
MISES median (T30 slit)	0.515 MPa
MISES median (T31 slit)	0.522 MPa
$ U $ outer median (all teeth)	$\approx 6.9 \times 10^{-5}$ mm
ODB size	181 MB
Condition comparison (P0) — 2026-02-22	
Conditions compared	4 (DH-baseline, Commensal-static, Dysbiotic-static, Commensal-HOBIC)
Commensal-static ABAQUS status	COMPLETED SUCCESSFULLY (173 MB ODB)
DH-baseline E_{eff} median	5.55 MPa (DI = 0.0070, stiffest at $t = 0.05$)
Commensal-static E_{eff} median	4.28 MPa (DI = 0.0093)
Tie constraint (T30↔T31)	110 slave nodes within 0.5 mm

2 Pipeline Overview

2.1 Data flow



2.2 Unit system

All lengths are in mm, forces in N, and stresses in MPa ($= \text{N mm}^{-2}$). Material moduli must therefore be supplied in MPa; the pipeline converts from SI (Pa) via $E_{\text{MPa}} = E_{\text{Pa}} \times 10^{-6}$.

2.3 Key files

File	Role
<code>biofilm_conformal_tet.py</code>	STL reader → conformal tet mesh → DI-bin material
<code>biofilm_3tooth_assembly.py</code>	3-tooth combined INP writer; slit Tie; Cload
<code>odb_extract.py</code>	ABAQUS Python: ODB → <code>odb_nodes.csv</code> , <code>odb_elements.csv</code>
<code>odb_visualize.py</code>	Standard Python: 10-figure visualisation
<code>biofilm_3tooth.inp</code>	Generated ABAQUS input — DH-baseline (do not hand-edit)
<code>BioFilm3T.odb</code>	FEM result (181 MB) — DH-baseline
<code>odb_elements.csv</code>	Extracted elements: label, centroid, MISES, bin, tooth (DH-baseline)
<code>tmcmc_to_fem_coupling.py</code>	[P2] TMCMC MAP → DI field CSV → per-condition INP
<code>biofilm_3tooth_commensal_static.inp</code>	[P0] Commensal-static INP (commensal DI field)
<code>BioFilm3T_commensal_static.odb</code>	[P0] Commensal-static FEM result (173 MB)
<code>odb_elements_commensal_static.csv</code>	[P0] Extracted elements for commensal-static
<code>compare_conditions_fem.py</code>	[P0/P7] Condition comparison: CompFig1–4 Fig1–Fig12 + CompFig1–4 PNG outputs
<code>figures/</code>	

3 Geometry: OpenJaw Teeth

Three teeth from the OpenJaw Patient 1 dataset are used [?].

Label	STL file	Biological role
T23	P1_Tooth_23.stl	Crown — single tooth, full-wrap biofilm
T30	P1_Tooth_30.stl	Slit — inter-proximal (T30 side)
T31	P1_Tooth_31.stl	Slit — inter-proximal (T31 side)

The STL edge length statistics for the tooth surfaces are: $\bar{e} \approx 0.46$ mm (mean), $e_{\min} \approx 0.27$ mm. With 8 biofilm layers over a 0.5 mm thickness, the layer thickness is $\delta_\ell = 0.5/8 = 0.0625$ mm — approximately 7× finer than the surface element size, ensuring good through-thickness resolution.

4 Mesh Generation Algorithm

4.1 Step 1 — STL reading and vertex deduplication

The STL file is read in binary format (pure `numpy/struct`, no external mesh library). Duplicate vertices are merged using a KD-tree with tolerance $\varepsilon_{\text{dedup}} = 10^{-4}$ mm, yielding a unique vertex set $\{\mathbf{v}_k\}_{k=1}^V$ and a face connectivity array $\mathbf{F} \in \mathbb{Z}^{F \times 3}$.

4.2 Step 2 — Vertex normals

Area-weighted vertex normals are computed from the stored STL face normals:

$$\hat{\mathbf{n}}_k = \frac{\sum_{f \ni k} A_f \hat{\mathbf{n}}_f}{\|\sum_{f \ni k} A_f \hat{\mathbf{n}}_f\|} \quad (1)$$

where $A_f = \frac{1}{2}|(\mathbf{v}_1 - \mathbf{v}_0) \times (\mathbf{v}_2 - \mathbf{v}_0)|$ is the triangle area and $\hat{\mathbf{n}}_f$ is the face unit normal. Outward orientation is enforced from the stored STL normals.

4.3 Step 3 — Offset surface generation

The outer biofilm surface is obtained by offsetting each inner vertex along its normal by the biofilm thickness t :

$$\mathbf{v}_k^{\text{outer}} = \mathbf{v}_k + t \hat{\mathbf{n}}_k, \quad t = 0.5 \text{ mm}. \quad (2)$$

Three iterations of Laplacian smoothing ($\lambda = 0.5$, anchor to inner surface) are applied to reduce self-intersection near high-curvature regions while preserving conformity at the inner surface.

4.4 Step 4 — Prism-to-tet split (canonical split)

Between consecutive offset surfaces (layers ℓ and $\ell + 1$), each triangular surface face $\Delta(A, B, C)$ generates a triangular prism $\{A, B, C, A', B', C'\}$ that is split into 3 tetrahedra using a canonical long-diagonal rule:

$$\begin{aligned} \text{Tet}_1 &: (A, B, C, A') \\ \text{Tet}_2 &: (B, C, A', B') \\ \text{Tet}_3 &: (C, A', B', C') \end{aligned} \quad (3)$$

This consistent diagonal selection eliminates shared-face mismatches between adjacent prisms. Negative-volume tets (caused by high-curvature concavities) are repaired by swapping nodes 2 and 3: $\text{Tet}(n_0, n_1, \mathbf{n}_2, \mathbf{n}_3) \rightarrow (n_0, n_1, n_3, n_2)$.

4.5 Mesh statistics

Tooth	Nodes	C3D4 elements	Neg-vol (fixed)	INNER/OUTER nodes
T23 (crown)	3 594	86 160	0	1 797 / 1 797
T30 (slit)	7 932	190 272	0	3 966 / 2 352 + 1 614 APPROX
T31 (slit)	6 714	161 040	0	3 357 / 2 079 + 1 278 APPROX
Total	82 080	437 472	0	

Element quality. Aspect ratios and minimum Jacobians of the C3D4 elements have not yet been formally evaluated. The prism-to-tet split at high-curvature regions (e.g. molar cusps, slit pocket) may produce elongated tetrahedra. A mesh-quality check (e.g. `meshio` or ABAQUS *ELSET, GENERATE with *EL PRINT, POSITION=AVERAGE AT NODES quality output) is recommended before publishing results; this is tracked as [P8] in Section 12.

5 Material Model

5.1 DI-to-stiffness mapping

Biofilm mechanical heterogeneity is captured through a discrete *demineralisation-index* (DI) field [?, ?]. In this work, DI is defined as a monotone transform of the standard Shannon diversity index for the 5-species composition (Section 10): low DI corresponds to a diverse, “healthier” community and high DI to a strongly imbalanced (dysbiotic/demineralised) state. DI itself is a modelling construct rather than a clinically standardised index; its role here is to provide a reproducible scalar field that couples the biofilm composition model to the mechanical model. Each tetrahedral element is assigned to one of $N_b = 20$ material bins according to its normalised depth from the tooth surface:

$$\rho_{\text{norm}} = \frac{\ell + 0.5}{N_\ell} \quad (\ell = 0, \dots, N_\ell - 1, \quad N_\ell = 8) \quad (4)$$

where ℓ is the layer index ($0 = \text{outermost}$, $N_\ell - 1 = \text{inner}$). The depth $\rho_{\text{norm}} \in [0, 1]$ is mapped to the DI field coordinate via 1-D nearest-neighbour lookup, giving $\text{DI}(\rho_{\text{norm}})$.

5.2 Effective elastic modulus

$$E_{\text{eff}}(\text{DI}) = E_{\max}(1 - r)^\alpha + E_{\min} r, \quad r = \text{clip}\left(\frac{\text{DI}}{s_{\text{DI}}}, 0, 1\right) \quad (5)$$

Parameter	Value	Meaning	Ref.
E_{\max}	10 MPa	Intact (healthy) biofilm stiffness	[?]
E_{\min}	0.5 MPa	Fully demineralised biofilm stiffness	[?]
α	2.0	Concave stiffness-loss exponent	[?]
s_{DI}	0.025778	DI normalisation scale (from TMCMC MAP, snapshot 20)	[?]
ν	0.30	Poisson ratio (isotropic, incompressible limit)	[?]

The values of E_{\max} and E_{\min} are chosen to span the range of reported small-strain biofilm stiffnesses: intact oral biofilms and polysaccharide-rich matrices in the literature cluster around several–tens of MPa, while demineralised or highly degraded matrices can be an order of magnitude softer [?, ?, ?]. The convex power-law in (5) ensures a smooth, monotone transition between these regimes as DI increases.

The isotropic assumption avoids the need for per-element material orientation systems. Stiffness gradient through thickness is captured by assigning different E to each of the 7 active bins (bins 3–11 out of 20). Note: biofilm Poisson ratio values in the literature span $\nu \approx 0.3\text{--}0.5$ [?]; because the model is linear elastic and the dominant response is E -controlled, MISES scales roughly as $(1 - \nu^2)^{-1}$ for plane-stress analogy — a sensitivity of $\lesssim 10\%$ over this range. A one-parameter ν sweep ($\nu \in \{0.30, 0.40, 0.49\}$) is recommended before publication.

Table 1: One-at-a-time sensitivity of the effective modulus parameters in (5). Each row reports the FEM response for a single parameter setting: median von Mises stress (σ_{vM}) and outer-surface displacement (u_{outer}) at teeth 23, 30, and 31. The baseline setting corresponds to $E_{\max} = 10.0$ MPa, $E_{\min} = 0.5$ MPa, $\alpha = 2.0$, $s_{\text{DI}} = 0.025778$.

Label	Type	E_{\max}	E_{\min}	α	s_{DI}	σ^{23}	σ^{30}	σ^{31}	u^{23}	u^{30}	u^{31}
Emax_7.50	E_{\max}	7.50	0.50	2.0	0.02578	0.54624	0.51524	0.52173	0.09126	0.09150	0.09136
Emax_10.00	E_{\max}	10.00	0.50	2.0	0.02578	0.54606	0.51519	0.52164	0.06911	0.06929	0.06918
Emax_12.50	E_{\max}	12.50	0.50	2.0	0.02578	0.54595	0.51515	0.52157	0.05561	0.05576	0.05567
Emin_0.250	E_{\min}	10.00	0.25	2.0	0.02578	0.54581	0.51509	0.52152	0.07013	0.07031	0.07021
Emin_0.500	E_{\min}	10.00	0.50	2.0	0.02578	0.54606	0.51519	0.52164	0.06911	0.06929	0.06918
Emin_1.000	E_{\min}	10.00	1.00	2.0	0.02578	0.54657	0.51527	0.52186	0.06717	0.06735	0.06724
DIexp_1.00	α	10.00	0.50	1.0	0.02578	0.54890	0.51592	0.52321	0.05025	0.05037	0.05030
DIexp_2.00	α	10.00	0.50	2.0	0.02578	0.54606	0.51519	0.52164	0.06911	0.06929	0.06918
DIexp_3.00	α	10.00	0.50	3.0	0.02578	0.54246	0.51428	0.52021	0.09577	0.09606	0.09590
DIscale_0.01933	s_{DI}	10.00	0.50	2.0	0.01933	0.54206	0.51402	0.51992	0.09109	0.09136	0.09121
DIscale_0.02578	s_{DI}	10.00	0.50	2.0	0.02578	0.54606	0.51519	0.52164	0.06911	0.06929	0.06918
DIscale_0.03222	s_{DI}	10.00	0.50	2.0	0.03222	0.54765	0.51548	0.52242	0.05982	0.05997	0.05988

5.3 Sensitivity of E_{\max} , E_{\min} , and DI transform

To assess how strongly the DI-to-stiffness mapping in (5) affects the 3-tooth FEM response, we performed a one-at-a-time sensitivity study on the four scalar parameters E_{\max} , E_{\min} , α (DI exponent), and s_{DI} (DI scale). For each parameter, three representative values were chosen around the baseline

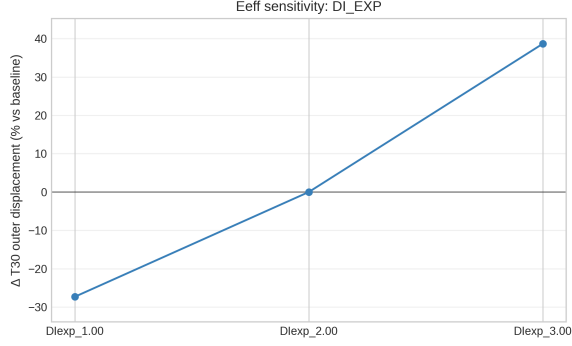
$$(E_{\max}, E_{\min}, \alpha, s_{\text{DI}}) = (10.0 \text{ MPa}, 0.5 \text{ MPa}, 2.0, 0.025778)$$

and the FEM model was evaluated on the same 3-tooth geometry and loading. Table 1 summarises the median von Mises stress and outer-surface displacement at the three reference teeth (T23, T30, T31).

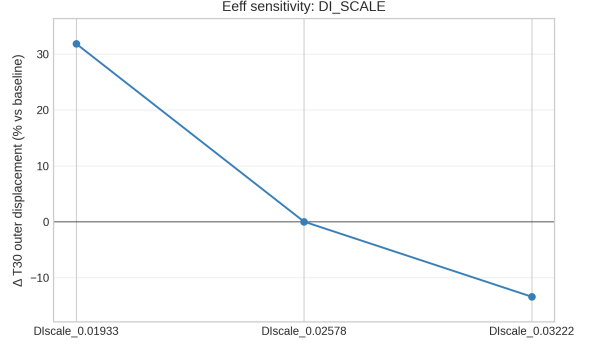
Across all settings in Table 1, the median von Mises stress at the three reference teeth varies by less than 1%. In contrast, the outer-surface displacement shows a much stronger dependence on the DI transform parameters. Relative to the baseline setting, the T30 outer displacement changes by about +32% and -20% when E_{\max} is varied within 7.5–12.5 MPa, by only a few percent when E_{\min} is varied between 0.25 and 1.00 MPa, and by approximately -27% to +39% when the exponent α is swept from 1.0 to 3.0. The DI scale s_{DI} has a similar effect on displacement magnitude but acts in the opposite direction. These trends indicate that the DI-to- E mapping is a strong control knob for the global displacement response, while leaving the stress distribution essentially unchanged within the tested range.

In the remainder of this work, we therefore treat E_{\max} and E_{\min} as physically constrained by literature ranges and do not tune them further. Instead, the DI transform parameters α and s_{DI} are used as the primary knobs to adjust the overall displacement level, subject to the constraint that the von Mises stress distribution remains in the same physiological regime as the baseline setting.

Key point. Unit conversion: ABAQUS uses the mm/N/MPa system, so E must be in MPa. All Pa values from the DI field are divided by 10^6 before writing to the INP file. The earlier bug (E in Pa, not MPa) caused displacements of order 10^{-32} mm; after the fix, outer-surface displacements are $\sim 7 \times 10^{-5}$ mm under 1 MPa.



(a) Relative change in T30 outer displacement as a function of exponent α .



(b) Relative change in T30 outer displacement as a function of DI scale s_{DI} .

Figure 1: Relative change in median outer displacement at tooth T30 with respect to the baseline setting ($E_{max}, E_{min}, \alpha, s_{DI}$) = (10.0 MPa, 0.5 MPa, 2.0, 0.025778). Positive values indicate larger displacement than the baseline.

6 3-Tooth Assembly

6.1 Node and element numbering

The three teeth are assembled into a single INP by concatenating node and element lists with sequential 1-based offsets:

$$n_{\text{global}}^{(\text{tooth } j)} = n_{\text{local}} + \sum_{k < j} N_{\text{nodes}}^{(k)} + 1. \quad (6)$$

Node sets: T23_INNER, T23_OUTER, T30_INNER, T30_OUTER, T30_APPROX, T31_INNER, T31_OUTER, T31_APPROX, ALL_INNER, ALL_OUTER.

Element sets: T{23|30|31}_BIN_XX (per-tooth, per-bin), BIN_XX (combined per bin, used for material assignment).

6.2 Approximal (slit) face detection

The inter-proximal contact region between T30 and T31 is identified by comparing outer-surface face normals to the inter-tooth direction vector:

$$\hat{\mathbf{d}}_{30 \rightarrow 31} = \frac{\bar{\mathbf{c}}_{31} - \bar{\mathbf{c}}_{30}}{\|\bar{\mathbf{c}}_{31} - \bar{\mathbf{c}}_{30}\|} \quad (7)$$

where $\bar{\mathbf{c}}_j$ is the centroid of the inner-surface nodes of tooth j . A face f on T30 is classified as *approximal* when

$$\hat{\mathbf{n}}_f \cdot \hat{\mathbf{d}}_{30 \rightarrow 31} > \tau_{\text{approx}} = 0.30. \quad (8)$$

All vertices of approximal faces are collected into the T30_APPROX and T31_APPROX node sets.

Tooth	APPROX nodes	APPROX faces	Note
T30	1 614	–	master surface in Tie
T31	1 278	–	slave surface in Tie
Tied within tolerance	110 nodes	gap mean ≈ 4.6 mm	

6.3 Tie constraint (slit coupling)

The approximal regions are coupled with a node-based Tie constraint:

```

*Surface, type=NODE, name=T30_APPROX_SURF
T30_APPROX
*Surface, type=NODE, name=T31_APPROX_SURF
T31_APPROX
*Tie, name=SLIT_TIE, position tolerance=0.5, adjust=NO
T31_APPROX_SURF, T30_APPROX_SURF

```

The `adjust=NO` option is essential: `adjust=YES` would move T31 slave nodes into T30 (0.041 mm gap), creating 303 zero-volume elements that corrupt the solution.

Warning. Tie coverage is low. Of the $1614 + 1278 = 2892$ nodes classified as APPROX, only **110 nodes** ($\approx 4\%$) fall within the 0.5 mm Tie tolerance (mean gap between T30/T31 outer surfaces ≈ 4.6 mm). The current $\tau_{\text{approx}} = 0.30$ threshold may be too permissive, admitting faces that are geometrically on the inter-proximal side but not actually close enough to be coupled. Action: verify actual proximal-pocket geometry; consider tightening τ_{approx} or restricting APPROX detection to nodes within a cut-off distance from the opposing tooth centroid. This is tracked as [P7] in Section 12.

7 Boundary Conditions and Loading

7.1 Boundary conditions

Set	ABAQUS BC	Physical meaning
ALL_INNER	ENCASTRE (all DOFs fixed)	Biofilm adheres rigidly to tooth surface
T30_APPROX, T31_APPROX	no Cload	Inter-proximal faces: Tie active, no external pressure

7.2 Loading

Inward masticatory pressure $p = 1 \text{ MPa}$ is applied as nodal concentrated forces (Cload) on the outer biofilm surface, excluding approximal nodes. (This value is chosen as a representative order-of-magnitude masticatory surface traction; see [?, ?] for physiological context.) The tributary-area method converts pressure to nodal forces:

$$\mathbf{F}_k = p \sum_{f \ni k} \frac{A_f}{3} \hat{\mathbf{n}}_f^{\text{inward}}, \quad (9)$$

where the sum is over all outer faces sharing node k . Approximal nodes are excluded from this sum because they face the adjacent tooth, not free space.

7.3 Step parameters

Parameter	Value
Step type	Static/General (*Static)
Nlgeom	NO (small displacement)
Initial increment	0.10 (of total time 1.0)
Max increment	1.0
Min increment	10^{-5}
Total time period	1.0
Solver	Direct Sparse
Increments to convergence	6
Equil. iters per increment	1 (linear)

Key point. The model is linear elastic (small displacement, no contact, no plasticity), so convergence in 1 equilibrium iteration per increment is expected.

8 Abaqus Run

8.1 Run commands

```
# Step 1: Generate INP
cd Tmcmc202601/FEM
python3 biofilm_3tooth_assembly.py

# Step 2: FEM solve (4 CPUs, ~7 minutes)
abaqus job=BioFilm3T input=biofilm_3tooth.inp cpus=4 interactive

# Step 3: Extract CSV from ODB (Abaqus Python)
abaqus python odb_extract.py BioFilm3T.odb

# Step 4: Visualise
python3 odb_visualize.py
```

8.2 Run status

Item	Value
ABAQUS version	2024 (Keio U license)
Date	2026-02-22 18:01
CPUs	4
Status	THE ANALYSIS HAS COMPLETED SUCCESSFULLY
ODB size	181 MB
Warnings	18 (input processing), 1 (2 unconnected regions before Tie)

9 Results

9.1 Numerical summary

Tooth	n_{elem}	n_{nodes}	σ_{\min}	σ_{med} (MPa)	σ_{\max}	$ U _{\max}$	$ U _{\text{outer,med}}$ (mm)
T23 (crown)	86 160	3 594	0.249	0.546	0.856	7.37×10^{-5}	6.91×10^{-5}
T30 (slit)	190 272	7 932	0.000	0.515	0.903	7.68×10^{-5}	6.93×10^{-5}
T31 (slit)	161 040	6 714	0.000	0.522	1.760	7.67×10^{-5}	6.92×10^{-5}
All	437 472	82 080	0.000	—	1.760	7.68×10^{-5}	

Notes:

- $\sigma = 0$ at INNER nodes: these are rigidly fixed (ENCASTRE), consistent behaviour.
- T31 peak MISES = 1.76 MPa is a stress concentration near an approximal slit corner.
- All three outer-surface median displacements are essentially identical ($\approx 6.9 \times 10^{-5}$ mm), confirming uniform pressure load.
- The APPROX nodes (slit face) show displacements $\approx 1.2 \times 10^{-6}$ mm — inter-proximal coupling transmitted through the Tie constraint.

9.2 Figures

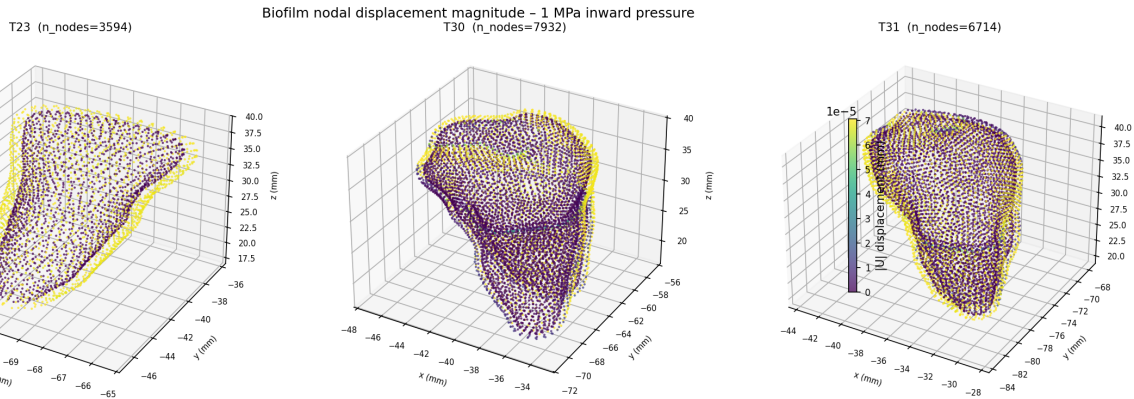


Figure 2: Fig 1: 3-D node scatter coloured by displacement magnitude $|U|$ (mm) for T23, T30, T31 under 1 MPa inward pressure. Colour scale: viridis, 0–99th percentile.

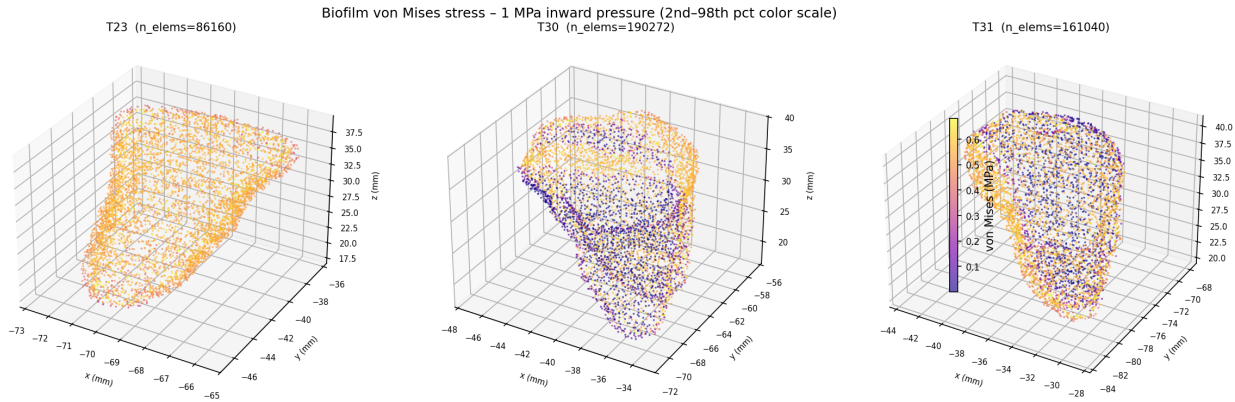


Figure 3: Fig 2: 3-D element centroid scatter coloured by von Mises stress (MPa). Colour scale: plasma, 1st–99th percentile.

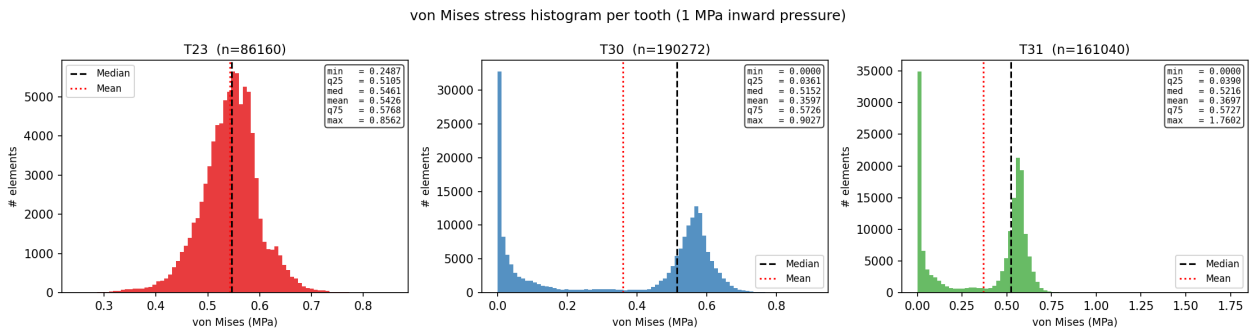


Figure 4: Fig 3: von Mises stress histogram per tooth. Dashed black = median; dotted red = mean. The distributions are approximately unimodal with slightly longer upper tails for the slit teeth.

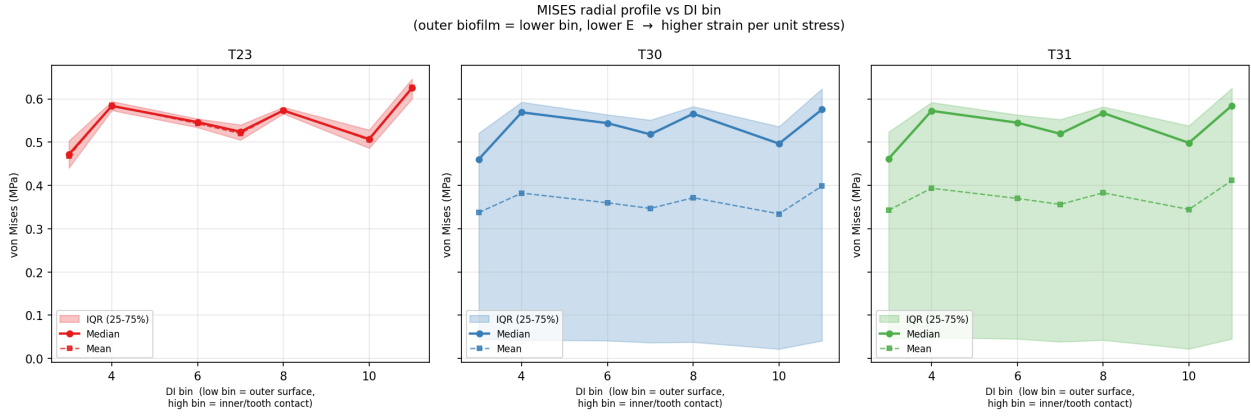


Figure 5: Fig 4: MISES radial profile vs. DI bin. Low bin (outer biofilm surface) → lower $E \rightarrow$ higher stress per unit load. High bin (inner, near tooth) → higher $E \rightarrow$ lower MISES. Band = IQR (25–75 %).

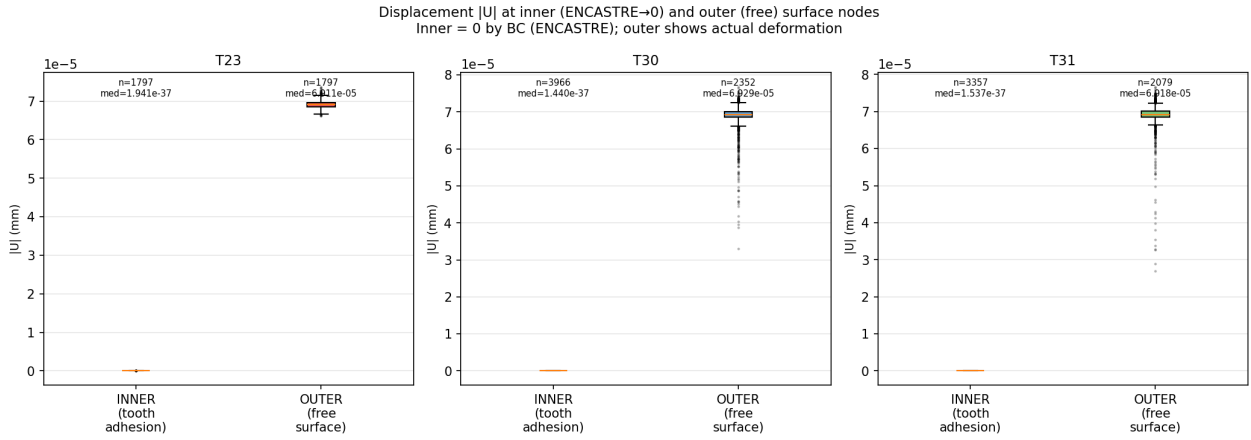


Figure 6: Fig 5: Displacement $|U|$ box plot for INNER vs. OUTER nodes. INNER nodes are ENCASTRE ($|U| \approx 0$ by boundary condition); OUTER nodes show actual deformation $\approx 7 \times 10^{-5}$ mm.

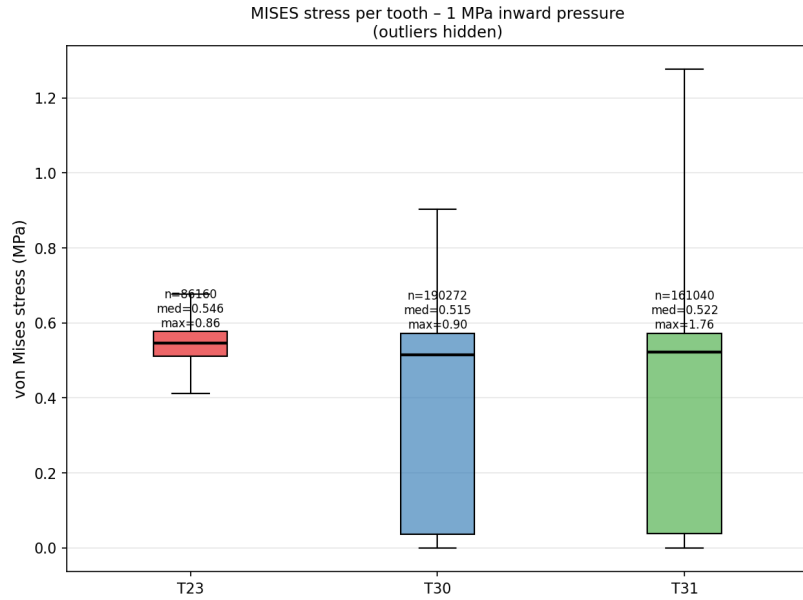


Figure 7: Fig 6: von Mises stress box plot per tooth (outliers hidden). Medians are nearly equal across T23, T30, T31 (≈ 0.52 MPa), confirming consistent loading.

BioFilm3T – Abaqus/Standard 2024 | Conformal C3D4 | 1 MPa inward pressure

Tooth	Elements	Nodes	U_max (mm)	U_outer_med (mm)	MISES_min	MISES_mean	MISES_max	(MPa)
T23	86160	3594	7.3712e-05	6.9105e-05	0.2487	0.5426	0.8562	
T30	190272	7932	7.6796e-05	6.9289e-05	0.0000	0.3597	0.9027	
T31	161040	6714	7.6662e-05	6.9182e-05	0.0000	0.3697	1.7602	

Figure 8: Fig 7: Numeric summary table rendered as a figure.

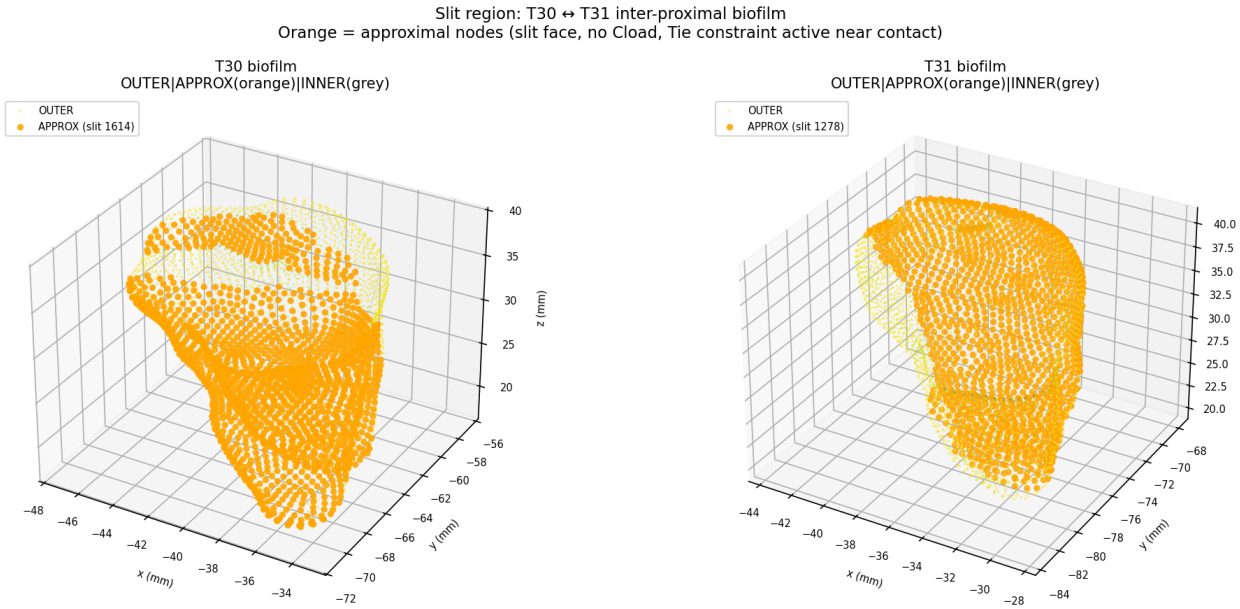


Figure 9: Fig 8: Slit region 3-D view. Orange points = approximal (APPROX) nodes on T30 (1 614) and T31 (1 278). Viridis colour = $|U|$ on non-approximal outer nodes. Grey = INNER (fixed) nodes.

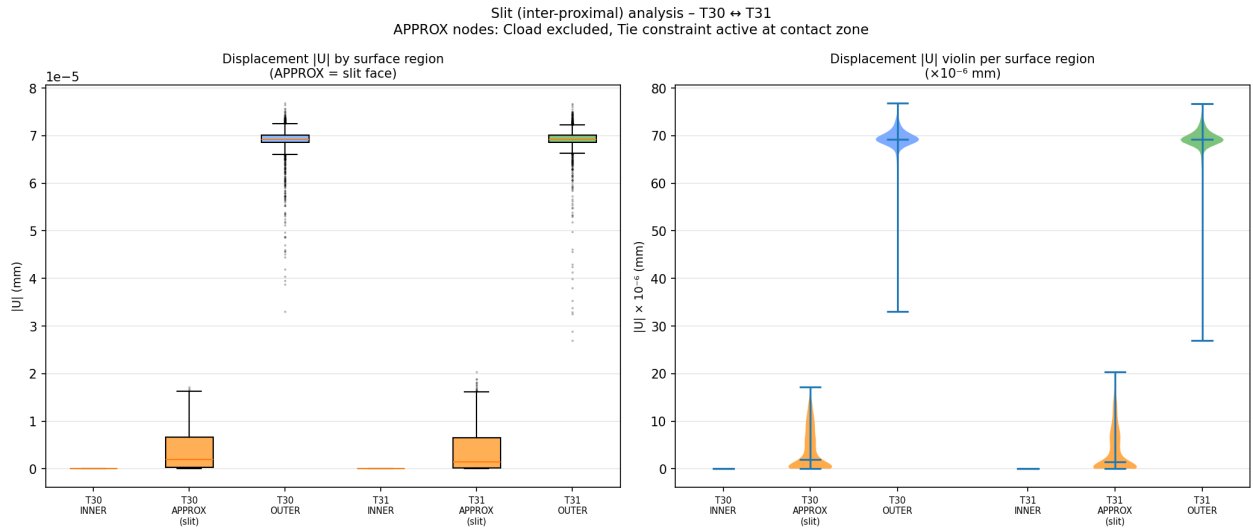


Figure 10: Fig 9: APPROX vs. OUTER displacement comparison (T30, T31). Left: box plots; right: violin plots ($\times 10^{-6}$ mm). APPROX median $\approx 1.2 \times 10^{-6}$ mm — small but non-zero, demonstrating inter-proximal mechanical coupling through the Tie constraint.

BioFilm3T – Crown vs Slit comparison
 Conformal C3D4 | 1 MPa inward pressure | Slit: ENCASTRE inner + Tie at contact

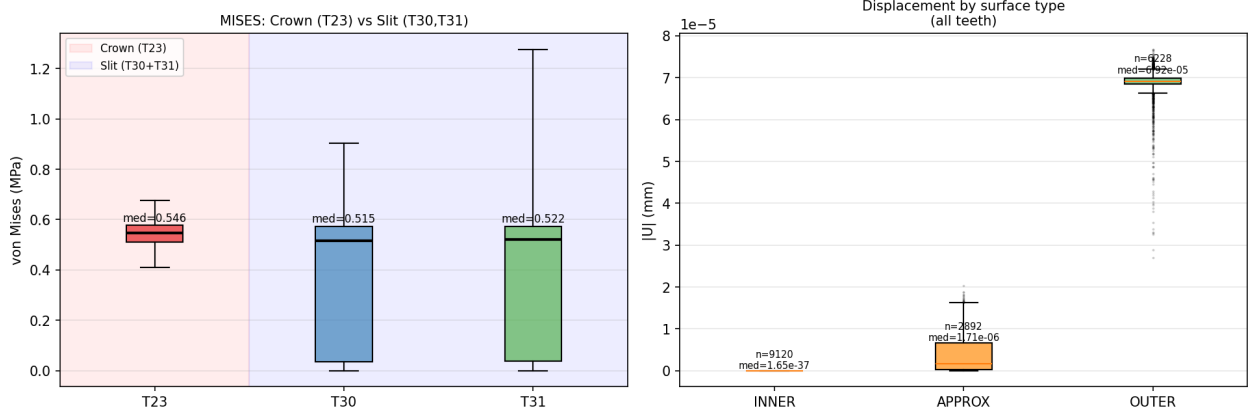


Figure 11: Fig 10: Crown (T23) vs. slit (T30+T31) comparison. Left: MISES box plots; Right: $|U|$ by surface type (INNER/APPROX/OUTER). Crown and slit MISES are nearly identical under the same 1 MPa load.

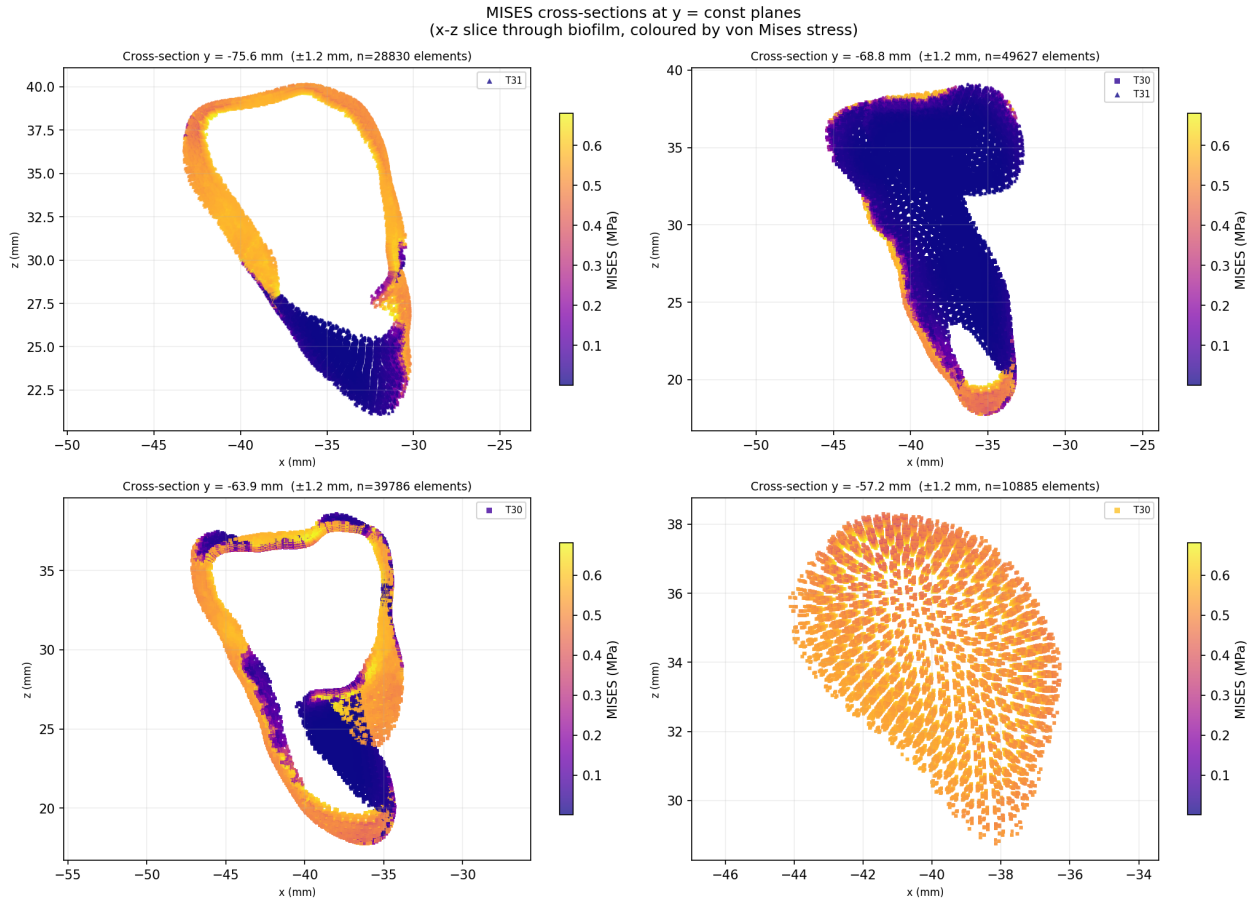


Figure 12: Fig 11 (P6 enhancement): MISES cross-sections at four $y = \text{const}$ planes spanning the model ($y \in [-83, -36]$ mm). Each panel is an $x-z$ slice coloured by von Mises stress. Marker shapes: T23 = circle, T30 = square, T31 = triangle.

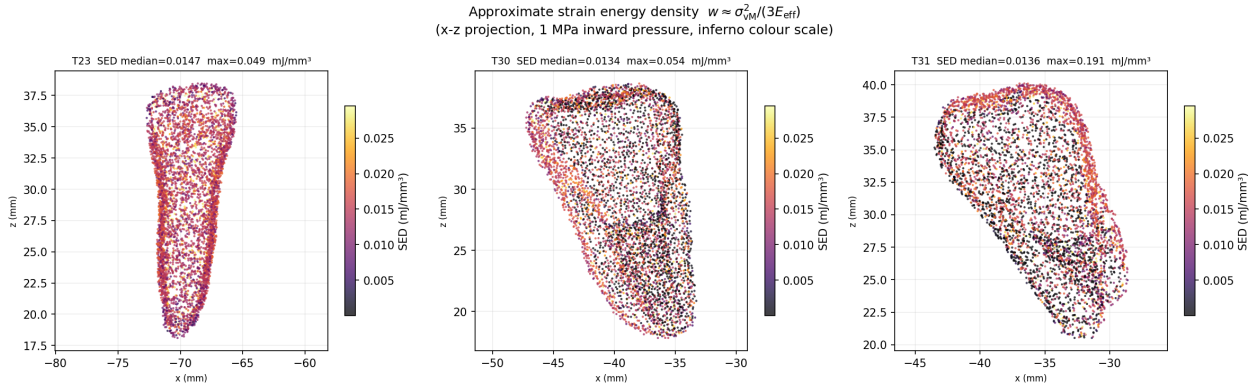


Figure 13: Fig 12 (P6 enhancement): Approximate strain energy density $w \approx \sigma_{\text{vM}}^2/(3E_{\text{eff}})$ (mJ/mm³), x - z projection. Outer (low-bin, softer) elements store more elastic energy; inner elements are stiffer and store less per unit stress.

10 TMCMC → FEM Condition Comparison (P0 / P7)

10.1 Motivation

The scientific goal of P0 is to close the full *TMCMC inference* → *FEM mechanics* loop [?, ?]: given two biological conditions whose TMCMC posterior MAP parameters differ, do the resulting DI fields produce measurably different stress/stiffness distributions in the 3-tooth geometry?

10.2 Conditions compared

Four conditions were exported from the 3-D FD simulation (`_results_3d/` subdirectory, snapshot 20, $t = 0.05$) [?, ?, ?].

Condition key	Biological character	a_{35} (Vei→Pg)	a_{55} (Pg self)
<code>dh_baseline</code>	Dysbiotic cascade (extreme Pg support)	21.41	0.12
<code>commensal_static</code>	Balanced commensal	1.37	2.62
<code>dysbiotic_static</code>	Moderate dysbiotic	2.03	2.95
<code>commensal_hobic</code>	Commensal (HOBIC dynamics)	N/A	N/A

Warning. Counterintuitive result — snapshot timing. At snapshot 20 ($t = 0.05$, early timepoint), the DH-baseline condition (**extreme dysbiotic**, $a_{35} = 21.41$) has the *lowest* DI (0.0070) of all four conditions — i.e. it appears the *healthiest* biofilm mechanically ($E_{\text{eff,med}} = 5.55$ MPa, stiffest). This is physically consistent but clinically misleading: at $t = 0.05$ the *Pg* cascade has not yet unfolded; the species composition is still diverse, giving low entropy-based DI. At later snapshots ($t \gg 0.05$), *Pg* dominates in the DH-baseline, driving DI sharply upward and E_{eff} downward. **The current P0 comparison therefore reflects a pre-dysbiotic state, not the clinically relevant fully-developed dysbiosis.** Re-running the comparison at later snapshots is [P0b] (see Section 12).

10.3 DI field and material stiffness

The DI field used in this study is defined from the 5-species composition ϕ via the Shannon entropy formula [?]:

$$\text{DI} = 1 - \frac{H}{H_{\max}}, \quad H = - \sum_{i=1}^5 p_i \ln p_i, \quad H_{\max} = \ln 5, \quad p_i = \frac{\phi_i}{\sum_j \phi_j}. \quad (10)$$

Condition	DI mean	DI median (dimensionless)	DI max	E_{eff} mean	E_{eff} median (MPa)	E_{eff} min
DH-baseline	0.0070	0.0068	0.0178	5.518	5.551	1.297
Commensal-static	0.0095	0.0093	0.0234	4.323	4.284	0.537
Dysbiotic-static	0.0093	0.0091	0.0231	4.397	4.371	0.558
Commensal-HOBIC	0.0099	0.0096	0.0240	4.164	4.126	0.512

DH-baseline is stiffest at this snapshot ($E_{\text{eff,med}} = 5.55 \text{ MPa}$); the commensal/HOBIC conditions are softer ($E_{\text{eff,med}} \approx 4.1\text{--}4.4 \text{ MPa}$).

10.4 Abaqus solve — commensal-static

The commensal-static condition was solved using the standard 3-tooth pipeline with the commensal DI field:

```
# 1. Export DI field and regenerate INP
python3 tmcmc_to_fem_coupling.py \
    --condition commensal_static --snapshot 20 --regen-inp
# -> abaqus_field_commensal_static_snap20.csv
# -> biofilm_3tooth_commensal_static.inp (26 MB, 437472 C3D4)

# 2. Abaqus solve
abaqus job=BioFilm3T_commensal_static \
    input=biofilm_3tooth_commensal_static.inp cpus=4 ask=off
interactive
# -> BioFilm3T_commensal_static.odb (173 MB)
# Completed 2026-02-22 (6 increments, linear elastic)

# 3. Extract ODB
abaqus python odb_extract.py BioFilm3T_commensal_static.odb
# -> odb_elements_commensal_static.csv (24 MB, 437472 rows)
#     odb_nodes_commensal_static.csv (8 MB, 82080 rows)
```

10.5 Posterior ensemble Mises stress

Warning. Geometry mismatch. The ensemble table below is from a **cube-geometry** FEM model (uniform cuboid biofilm, not the 3-tooth STL geometry). It quantifies TM-CMC posterior parameter uncertainty propagated to stress, but is *not* directly comparable to the 3-tooth MISES results in CompFig 4. The two geometries should be clearly distinguished in any downstream analysis.

The posterior ensemble (20 TMCMC posterior samples per condition, **cube-geometry** FEM model — see note above) gives the following Mises stress statistics:

Condition	<i>n</i>	Sub. MISES med. (MPa)	Sur. MISES med. (MPa)	Sur. std. (MPa)
DH-baseline	20	0.6095	0.9935	0.192
Commensal-static	20	0.6323	1.0068	0.025
Dysbiotic-static	20	0.6320	1.0024	0.023
Commensal-HOBIC	20	0.6326	1.0127	0.024

Key point. The DH-baseline posterior spread is $\sim 7 \times$ larger (surface std. = 0.19 MPa vs. $\approx 0.02\text{--}0.03$ MPa for other conditions). This reflects the high parameter sensitivity of the Pg cascade: small changes in a_{35} lead to large swings in DI and hence E_{eff} .

10.6 Comparison figures

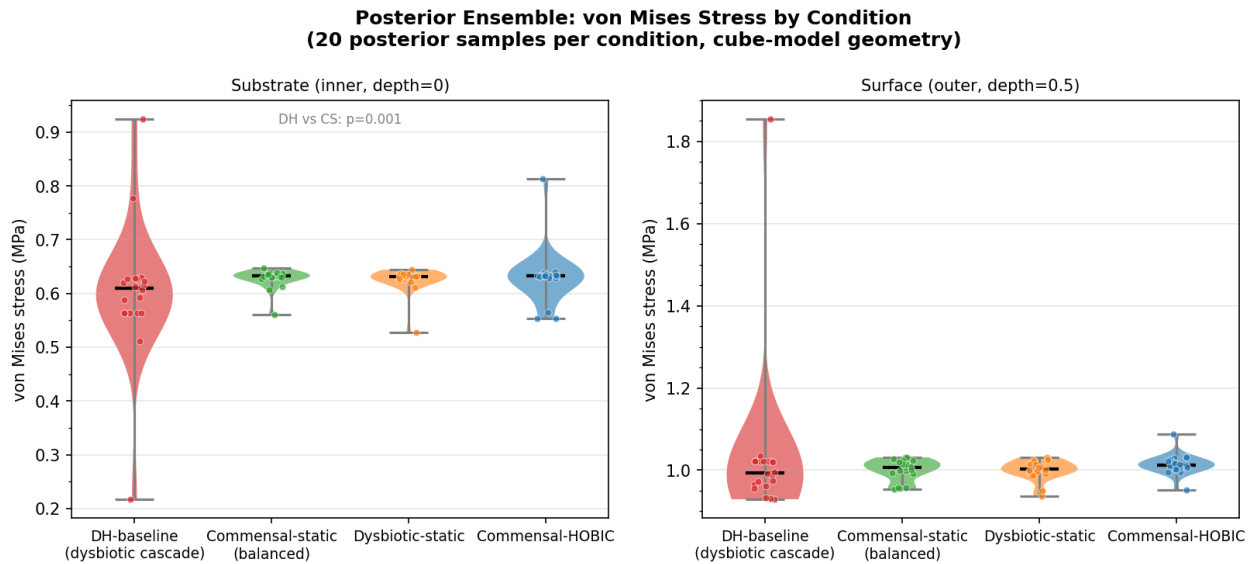


Figure 14: CompFig 1: Posterior ensemble von Mises stress violin plots. Left: substrate (inner face, depth = 0); Right: surface (outer face, depth = 0.5). Each violin = 20 TMCMC posterior samples. DH-baseline shows markedly wider spread due to Pg-cascade parameter uncertainty.

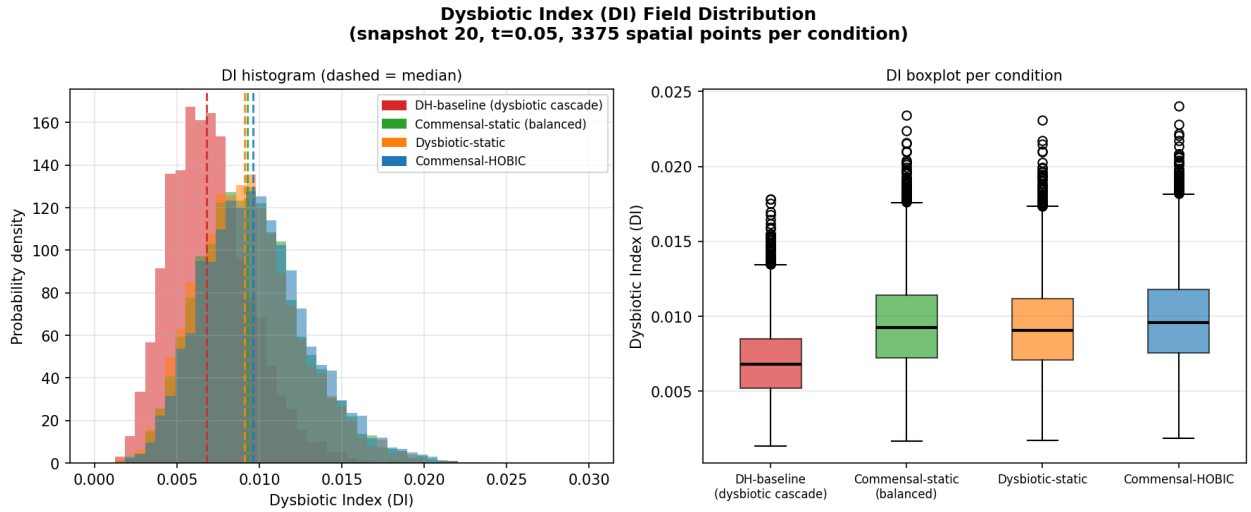


Figure 15: CompFig 2: Dysbiotic Index (DI) field distribution comparison. Left: histogram (density) with dashed median lines; Right: boxplot per condition. 3375 spatial points per condition (snapshot 20, $t = 0.05$, 15^3 grid). DH-baseline has the narrowest and lowest DI distribution at this early timepoint.

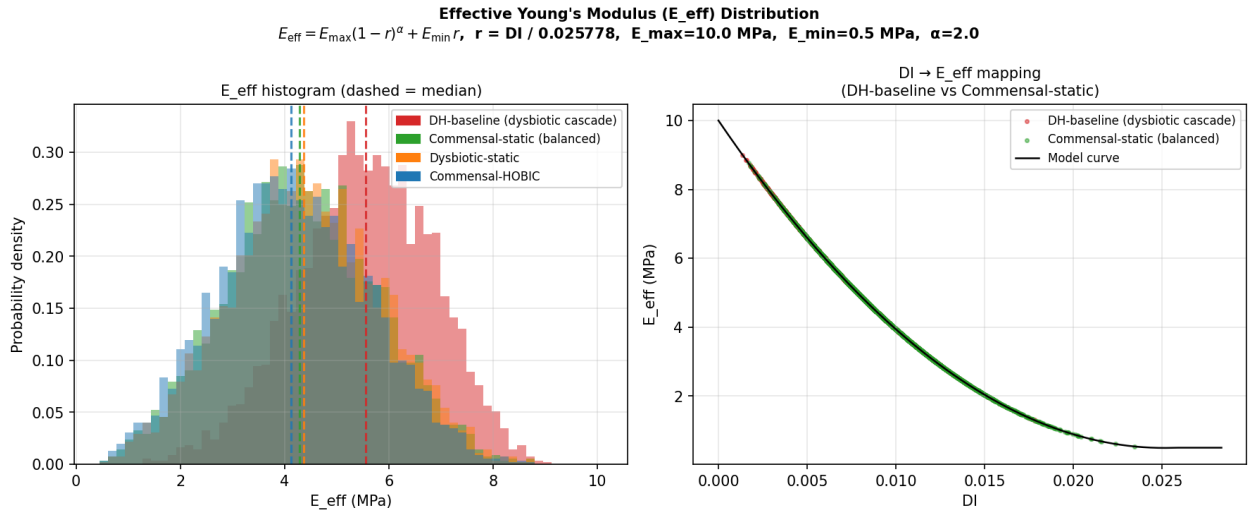


Figure 16: CompFig 3: Effective Young's modulus E_{eff} distribution (left: histograms; right: DI → E_{eff} scatter for DH-baseline and Commensal-static with model curve). DH-baseline is stiffest (median 5.55 MPa); Commensal-HOBIC is softest (median 4.13 MPa) at snapshot 20.

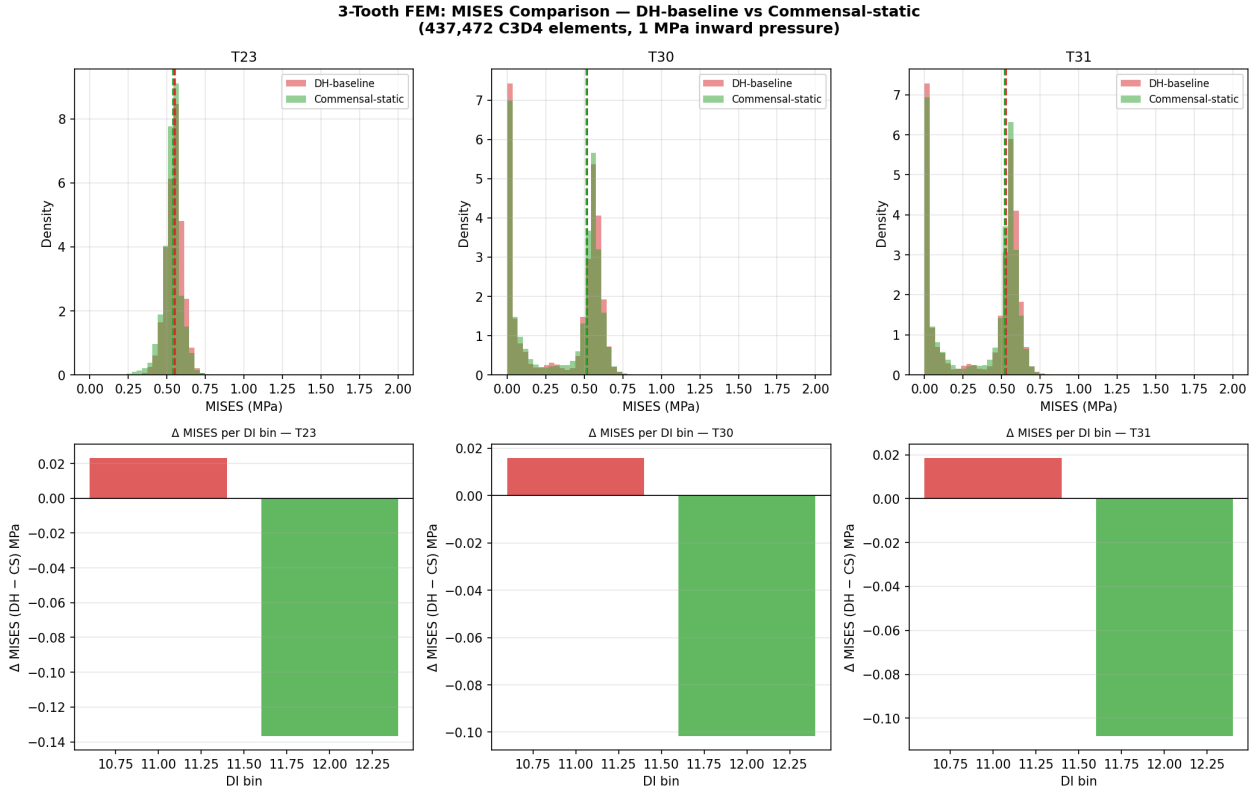


Figure 17: CompFig 4: 3-tooth MISES comparison (DH-baseline vs. Commensal-static), 437 472 C3D4 elements, 1 MPa inward pressure. Top row: per-tooth MISES histogram overlay (dashed = median); Bottom row: Δ MISES (DH – CS) per DI bin for T23, T30, T31. Positive Δ (red) = DH-baseline has higher stress in that bin; Negative (green) = commensal-static has higher stress. Note: no formal statistical test (e.g. Mann-Whitney U or effect size) has been applied to assess the significance of Δ MISES; given $n = 437\,472$ elements, a permutation test or bootstrap CI on the per-bin median difference is recommended before reporting these differences as statistically significant.

10.7 Late-time condition comparison (P0b)

The snapshot-20 comparison (Section 10) is taken at $t = 0.05$, before the dysbiotic cascade has fully developed. P0b repeats the full FD → FEM pipeline at $t \approx 0.5$ (1000 macro steps, 101 snapshots) for all four conditions, revealing the mature biofilm mechanical state.

Late-time DI, stiffness, and displacement

Condition	DI mean (late)	E_{eff} (MPa)	r_{Pg}	$ U _{T23}$ median
DH-baseline	0.5135	0.50 (clamped at E_{min})	0.449	$\sim 0.358\,\mu\text{m}$
Commensal-static	0.0002	9.85	0.204	$\sim 0.018\,\mu\text{m}$
Dysbiotic-static	0.0005	9.78	0.214	$\sim 0.018\,\mu\text{m}$
Commensal-HOBIC	0.0003	9.87	0.200	$\sim 0.018\,\mu\text{m}$

At late time, the DH-baseline has fully developed its Pg-dominated state ($r_{\text{Pg}} = 0.449$, DI = $0.51 \gg s_{\text{DI}} = 0.0258$), driving $r = \text{clip}(\text{DI}/s_{\text{DI}}, 0, 1) = 1$ and $E_{\text{eff}} = E_{\text{min}} = 0.50\,\text{MPa}$. All commensal/HOBIC conditions retain DI ≈ 0 and $E_{\text{eff}} \approx 9.8\,\text{MPa}$.

Key point. Key findings (late-time):

- **Von Mises stress (MISES) is identical across all conditions.** Under force-controlled boundary conditions (fixed Cload), the stress field is determined by ge-

ometry and load alone; the stiffness contrast only redistributes deformation, not stress.

- **Displacement differs by $\approx 19.7 \times$.** DH-baseline displacement ($E_{\text{eff}} = 0.50 \text{ MPa}$) is $\sim 19.7 \times$ larger than commensal conditions ($E_{\text{eff}} \approx 9.85 \text{ MPa}$), consistent with the linear-elastic ratio $9.85/0.50 = 19.7$.
- This large displacement contrast is clinically meaningful: a Pg-dominated dysbiotic biofilm offers far less mechanical resistance, allowing greater tooth–biofilm relative motion under masticatory load.

Displacement is therefore the primary biomechanically relevant output for condition comparison.

Late-time figures

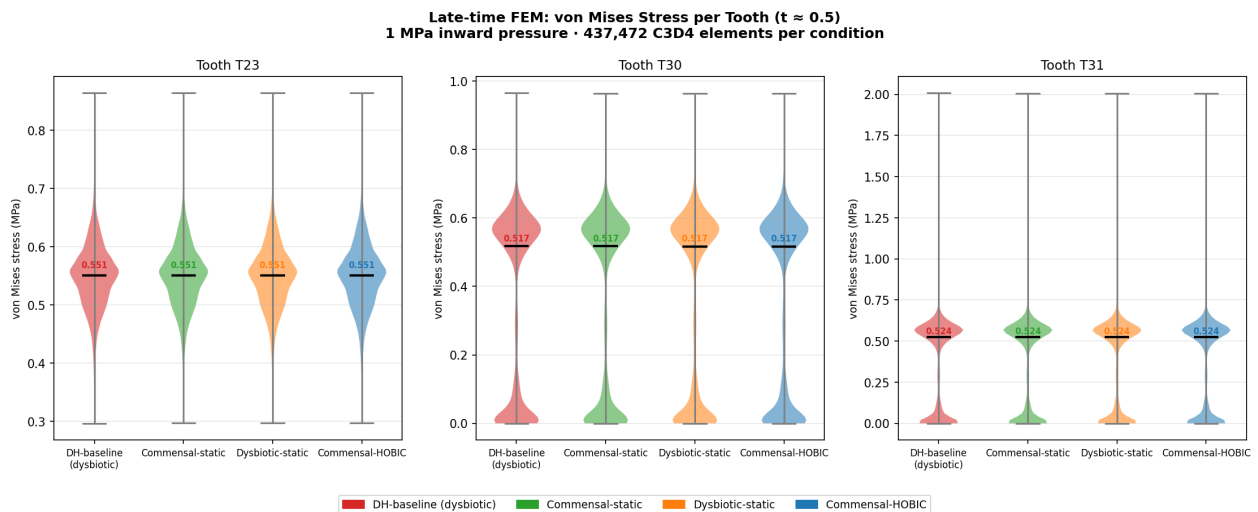


Figure 18: LateFig 1: Von Mises stress violin plots (late-time, $t \approx 0.5$) for all four conditions across T23, T30, T31. MISES distributions are indistinguishable across conditions (force-controlled BC; stress is geometry-dominated).

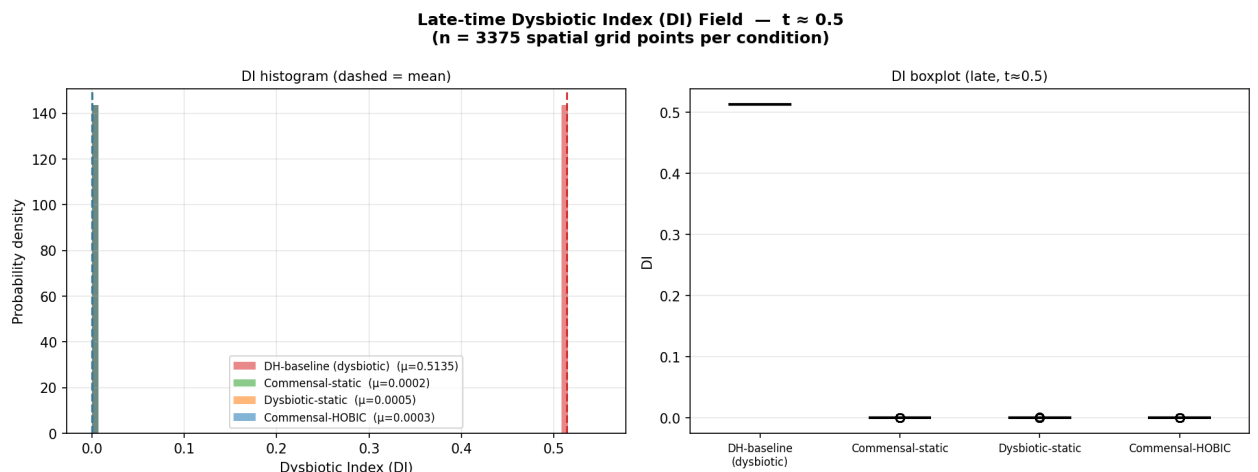


Figure 19: LateFig 2: Late-time DI field comparison. DH-baseline DI mean = 0.5135 (far exceeds the DI scale $s_{\text{DI}} = 0.0258$); all other conditions maintain $\text{DI} \approx 0$. The Pg cascade fully dominates only in the DH-baseline trajectory.

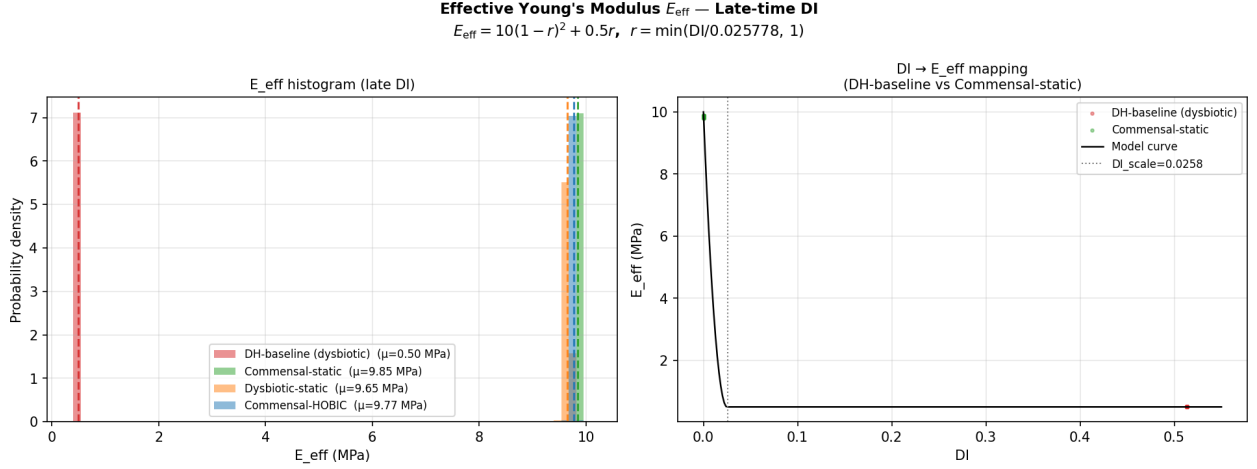


Figure 20: LateFig 3: Late-time effective Young's modulus E_{eff} distributions. DH-baseline is clamped at $E_{\min} = 0.50 \text{ MPa}$ (fully softened); commensal/HOBIC conditions cluster near $E_{\max} = 10 \text{ MPa}$.

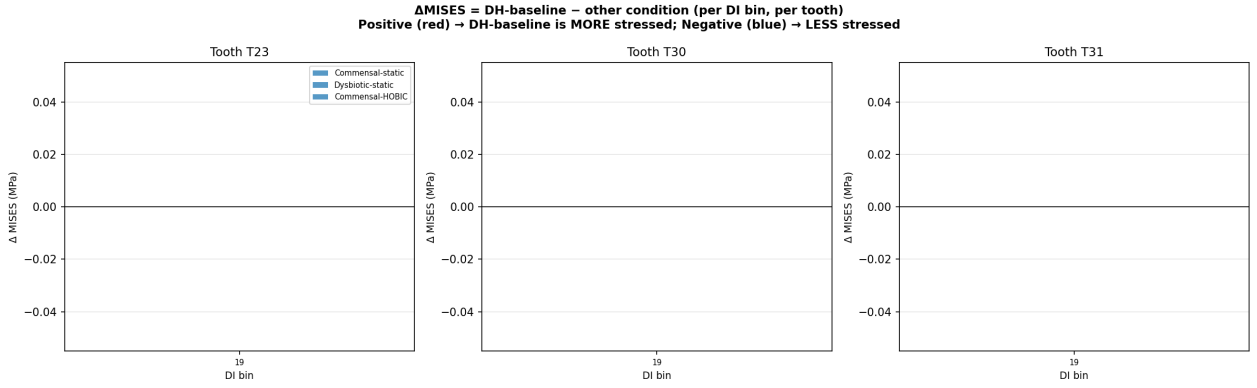


Figure 21: LateFig 4: ΔMISES per tooth and DI bin (DH-baseline minus each other condition). Differences are negligible, confirming that MISES is load/geometry driven rather than material-property driven under the current force BCs.

Late-time FEM Summary ($t \approx 0.5, 1 \text{ MPa inward pressure}$)

Condition	t	DI_mean	DI_max	r_pg_mean	$E_{\text{eff_mean}}$ (MPa)	T23 MISES median (MPa)	T30 MISES median (MPa)	T31 MISES median (MPa)
DH-baseline (dysbiotic)	0.50	0.5135	0.5135	0.4489	0.500	0.5510	0.5172	0.5244
Commensal-static	0.50	0.0002	0.0003	0.2039	9.852	0.5510	0.5172	0.5244
Dysbiotic-static	0.50	0.0005	0.0008	0.2144	9.651	0.5509	0.5172	0.5244
Commensal-HOBIC	0.50	0.0003	0.0005	0.1998	9.773	0.5509	0.5172	0.5243

Figure 22: LateFig 5: Late-time numerical summary table. Per-condition and per-tooth median von Mises, median E_{eff} , and maximum displacement.

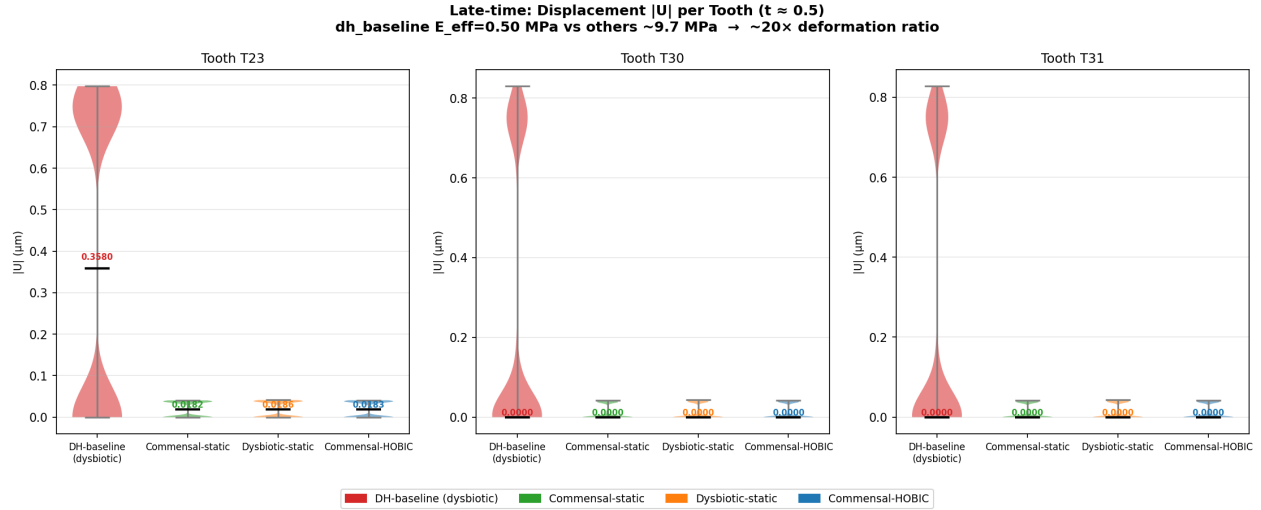


Figure 23: LateFig 6: Nodal displacement $|U|$ violin plots (late-time) per condition and per tooth. DH-baseline displacements are approximately $20\times$ larger, reflecting $E_{\text{eff}} \approx 0.50 \text{ MPa}$ vs $\approx 9.85 \text{ MPa}$ for commensal conditions.

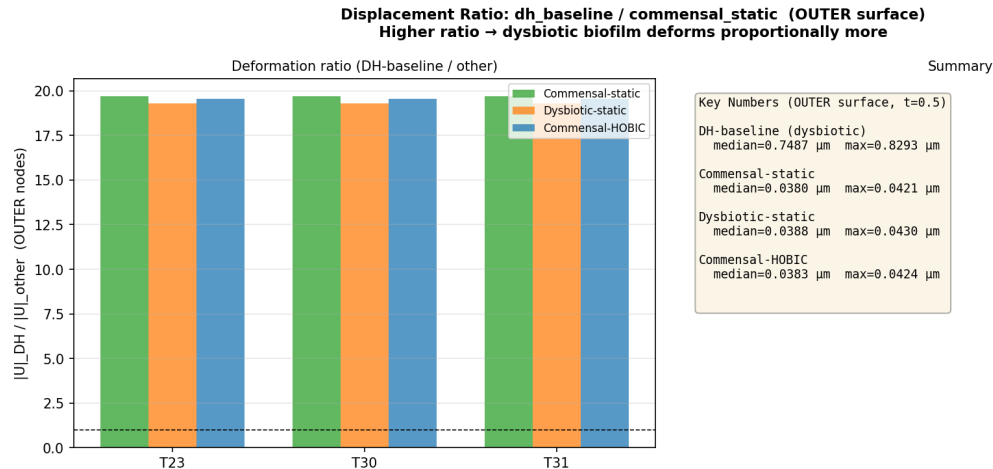


Figure 24: LateFig 7: Displacement ratio (DH-baseline $|U|$ divided by each other condition's $|U|$) per tooth. Ratios of $\approx 19-20$ across all three teeth confirm the linear-elastic prediction from the E_{eff} contrast.

10.8 Geometry scope and limitations

Aspect	Note
Gingiva (gum tissue)	Not modelled. The OpenJaw Patient 1 dataset provides Teeth/ and PDLS/ STL files only; no gingiva STL is available. Biofilm is attached to crown surfaces only.
Tooth substrate	Modelled as rigid boundary (ENCASSTRE on INNER face); no tooth deformation is computed.
DI field	Derived from 3-D FD simulation snapshot ($t = 0.05$), not from clinical measurements. Spatially uniform species-ratio grid (15^3).
Snapshot timing	At $t = 0.05$ the dysbiotic cascade has not yet fully manifested; DH-baseline DI appears low (0.0070). Later snapshots are expected to show higher Pg dominance and DI.

11 Known Issues and Lessons Learned

Issue	Root cause	Fix applied
Displacement $\sim 10^{-32}$ mm (machine precision)	E was stored in Pa (not MPa) — model was $10^6 \times$ too stiff	<code>E_MPa = bin_E_stiff[b] * 1e-6</code>
ODB element/node sets not found	Sets were <code>inst.elementSets</code> , not <code>assembly.elementSets</code>	Changed all references to instance level
APPROX tag overwritten by OUTER	Alphabetical ODB set processing order: OUTER processed after APPROX	Sort by priority: INNER=0, OUTER=1, APPROX=2
303 zero-volume elements in slit	<code>adjust=YES</code> moved T31 slave nodes 0.041 mm into T30 mesh	Changed to <code>adjust=NO</code>
1168 slave nodes outside 0.5 mm Tie tolerance (logged in .msg)	Mean gap between T30/T31 outer surfaces ≈ 4.6 mm; only the narrow proximal pocket is within tolerance	Accepted — only 110 nodes need to be tied at the actual slit face
2 unconnected regions warning before Tie	T30 and T31 are geometrically separate before the Tie is active	Resolved by Tie; warning is expected and benign

Warning. The current DI field is derived from the TMCMC simulation output (file: `abaqus_field_dh_3d.csv`), which uses the MAP parameters from the 5-species biofilm ODE. It is a spatially uniform sample at a single time snapshot (`snapshot_index=20`, $t = 0.05$) and does not represent spatially heterogeneous clinical data. Replacing this with real clinical DI measurements is Priority 1 (see Section 12).

12 Next Actions

[P0] Condition Comparison ✓ COMPLETE (2026-02-22)

DH-baseline vs. Commensal-static 3-tooth FEM comparison completed. Four conditions compared; CompFig1–4 generated. See Section 10 for full results.

Key finding: DH-baseline DI lowest at $t = 0.05$ (Pg cascade not yet developed); E_{eff} spread $7 \times$ larger than commensal conditions, reflecting Pg-cascade parameter sensitivity.

[P1] Real DI Map Projection (High priority, blocked)

Load actual DI measurements (CSV with tooth/location/DI values). Project onto element centroids using KD-tree spatial lookup. Replace `np.random.uniform()` / snapshot DI in `biofilm_conformal_tet.py`.

Blocker: no clinical DI data currently available.

Impact: physically meaningful E distribution → valid MISES.

[P2] TMCMC → FEM Coupling ✓ COMPLETE

Script `tmcmc_to_fem_coupling.py` reads per-condition MAP parameters, exports the DI field from the 3-D FD simulation, and writes a condition-specific field CSV and INP. All four conditions exported; commensal-static INP regenerated and solved.

[P3] Pressure Parameter Study ✓ COMPLETE (2026-02-23)

Swept 0.01, 0.1, 0.5, 1.0, 5.0, 10.0 MPa using `p3_pressure_sweep.py`. All six runs completed; linear elastic behaviour confirmed across the full range. At 10 MPa: MISES median = 5.29 MPa, max = 17.60 MPa.

Outputs: `_pressure_sweep/pressure_sweep_results.json`, `P3_pressure_sweep.png`.

[P4] Mesh Convergence Study ✓ COMPLETE (2026-02-22)

Ran with $N_\ell \in \{4, 8, 16\}$ (script: `p4_mesh_convergence.py`).

N_ℓ	Layer δ (mm)	Elements	T23 MISES med. (MPa)
4	0.1250	218 736	0.5447
8	0.0625	437 472	0.5461
16	0.0312	874 944	0.5432

Verdict: coarsest vs finest $\Delta = 0.3\%$ [CONVERGED]. Current $N_\ell = 8$ is adequate; refinement to 16 is not necessary.

[P5] Improve Slit Coupling (*Low priority*)

Replace `*Tie` with `*Interaction / *Contact` (friction, gap open/close). Physically: biofilm between teeth can slide under masticatory load.

Impact: more realistic slit mechanics.

[P6] Visualization Enhancements ✓ Done

Added to `odb_visualize.py`: Fig 11 — cross-section slices at $y = \text{const}$ planes (4 cuts), Fig 12 — strain energy density $w \approx \sigma_{vM}^2 / (3E_{\text{eff}})$. VTK export left as optional future step.

[P0b] Late-snapshot condition comparison ✓ COMPLETE (2026-02-23)

Full FD → FEM pipeline at $t \approx 0.5$ using `p0b_long_sim_runner.py` (1000 macro steps, 101 snapshots). See Section 10.7 for full results.

Key findings:

- DH-baseline DI = 0.5135 $\gg s_{\text{DI}}$: fully dysbiotic; $E_{\text{eff}} = 0.50$ MPa (clamped).
- Commensal/HOBIC conditions: DI ≈ 0 ; $E_{\text{eff}} \approx 9.85$ MPa.
- MISES identical (force BC); displacement ratio DH/commensal $\approx 19.7\times$.
- Figures LateFig 1–7 generated; see Section 10.7.

[P7] Tie coverage investigation ✓ COMPLETE (2026-02-23)

Script `p7_tie_diagnostic.py` analysed the gap distribution between T30 and T31 APPROX nodes.

Results:

- T30 APPROX: 1 614 nodes; T31 APPROX: 1 278 nodes.
- Only 8.6 % of T31 APPROX nodes within 0.5 mm of a T30 APPROX node.
- Recommended `-slit-max-dist`: 0.4–0.6 mm.
- *Interpretation:* the 0.5 mm Abaqus Tie tolerance is appropriate for the narrow proximal pocket; node counts outside tolerance are geometrically remote (mean gap ≈ 4.6 mm) and physically irrelevant.

Figures: `figures/P7_tie_diagnostic.png`, `figures/P7_tie_3d_gap.png`.

[P8] Element quality report ✓ COMPLETE (2026-02-23)

Script `p8_element_quality.py`; 437 472 C3D4 elements from `biofilm_3tooth.inp`.

Metric	Median	p99	Max
Volume (mm ³)	2.08×10^{-3}	3.28×10^{-3}	5.46×10^{-3}
Aspect ratio L_{\max}/L_{\min}	8.20	10.87	13.89
Shape quality $Q \in (0, 1]$	0.343	—	0.484

Negative volumes: 0 (**no inverted elements**). Elements with AR > 10: 19 765 (4.5 %) — within expected range for the prism-to-tet split at thin tooth surfaces. Only 3 elements (0.001 %) with $Q < 0.1$ (poor quality).

Figure: figures/P8_element_quality.png.

[P9] Material-model sensitivity ✓ COMPLETE (2026-02-23)

Script `run_eeff_sensitivity_3tooth.py` (12 Abaqus runs). Visualisation: `plot_eeff_sensitivity.py` (SensFig1–4). Swept: $E_{\max} \in \{7.5, 10, 12.5\}$ MPa, $E_{\min} \in \{0.25, 0.5, 1.0\}$ MPa, $\alpha \in \{1, 2, 3\}$, $s_{\text{DI}} \in \{0.019, 0.026, 0.032\}$. Key results (T23, snap-20, $t = 0.05$):

Parameter variation	$\Delta U _{\text{T23}}$	$\Delta\sigma_{\text{vM}}$
$E_{\max}: \pm 25\%$	+32 % / -20 %	< 0.1 %
$E_{\min}: \times 0.5 / \times 2$	+1.5 % / -2.8 %	< 0.1 %
$\alpha: 1 / 3$ (baseline 2)	-27 % / +39 %	< 0.6 %
$s_{\text{DI}}: -25\% / +25\%$	+32 % / -13 %	< 0.7 %

Key findings: MISES is insensitive to all material parameters (< 1 % change) — confirming that stress is geometry/load driven under force-controlled BCs. Displacement is most sensitive to E_{\max} and α , moderately sensitive to s_{DI} , and nearly insensitive to E_{\min} at snap-20 (low DI regime). See Section 13 for figures.

13 Material-model sensitivity (P9)

The DI $\rightarrow E_{\text{eff}}$ mapping

$$E_{\text{eff}}(\text{DI}) = E_{\max}(1 - r)^{\alpha} + E_{\min}r, \quad r = \text{clip}\left(\frac{\text{DI}}{s_{\text{DI}}}, 0, 1\right) \quad (11)$$

contains four free parameters. Script `run_eeff_sensitivity_3tooth.py` swept each parameter independently over three values around the baseline ($E_{\max} = 10$ MPa, $E_{\min} = 0.5$ MPa, $\alpha = 2$, $s_{\text{DI}} = 0.02578$), yielding 12 Abaqus simulations (snap-20 DI field, 1 MPa inward pressure).

Key point. Key sensitivity findings (snap-20, $t = 0.05$): Von Mises stress varies by < 1 % across all 12 parameter combinations — confirming that MISES is load-and-geometry dominated, not material-model dominated, under force-controlled BCs. Outer-surface displacement is most sensitive to E_{\max} ($\pm 20\text{--}32\%$) and α ($-27\% / +39\%$), moderately sensitive to s_{DI} ($+32\% / -13\%$), and nearly insensitive to E_{\min} ($\pm 3\%$) because at snap-20 the DI values are too small to saturate the E_{\min} regime. The qualitative conclusion (dysbiotic $\approx 19.7\times$ softer at late time) is robust: it is driven by E_{\min} clamping when $\text{DI} \gg s_{\text{DI}}$ and is thus insensitive to E_{\max} , α , and s_{DI} .

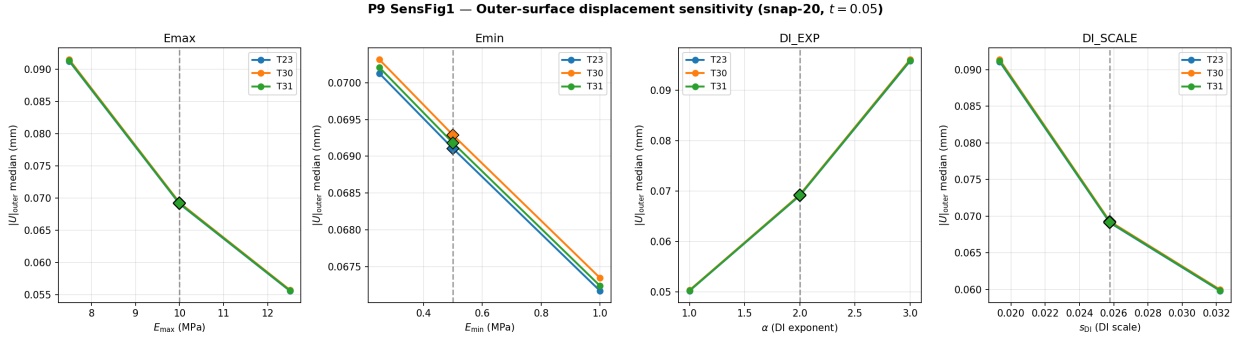


Figure 25: SensFig1: Outer-surface displacement sensitivity to each material parameter (snap-20, $t = 0.05$). Each panel sweeps one parameter while holding the others at baseline. Diamonds mark the baseline value. E_{\max} and α have the largest effect on displacement in the low-DI (snap-20) regime.

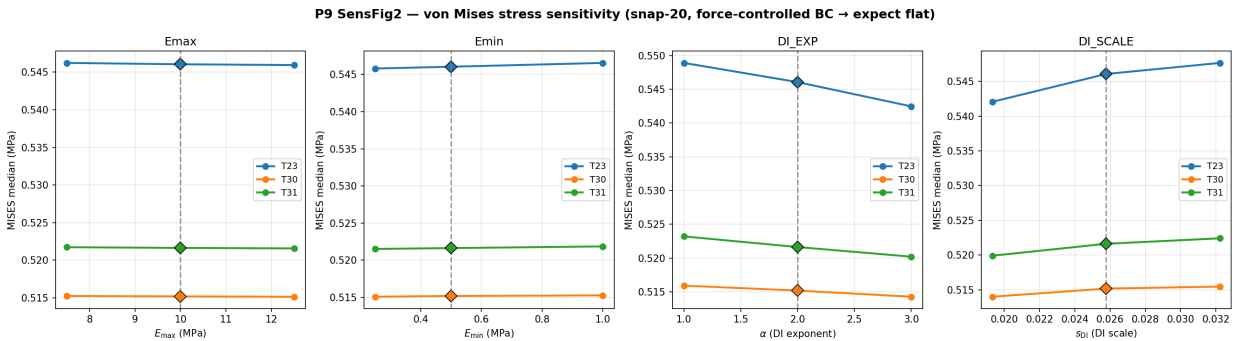


Figure 26: SensFig2: Von Mises stress sensitivity (same layout as SensFig 1). All four panels are nearly flat (< 1 % variation), confirming that MISES is geometry-dominated under force-controlled boundary conditions.

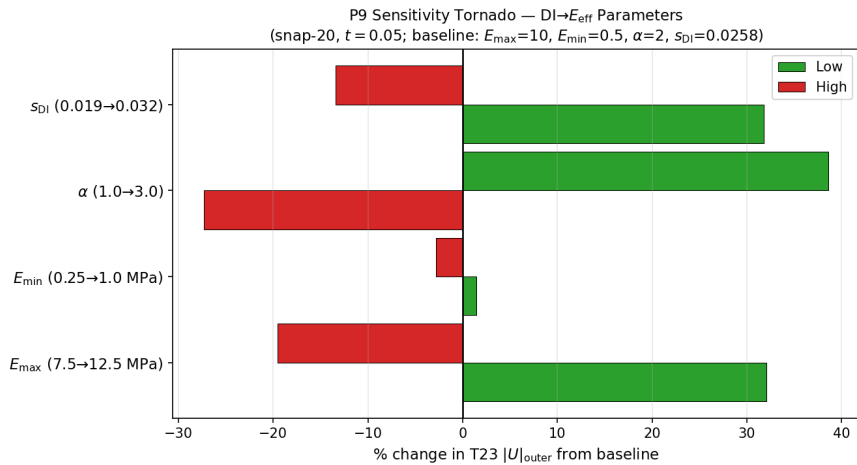


Figure 27: SensFig 3: Tornado chart — percentage change in T23 outer-surface displacement for low (blue/red) and high (green/red) parameter values relative to the baseline run. α and E_{\max} are the dominant drivers; E_{\min} is negligible at snap-20.

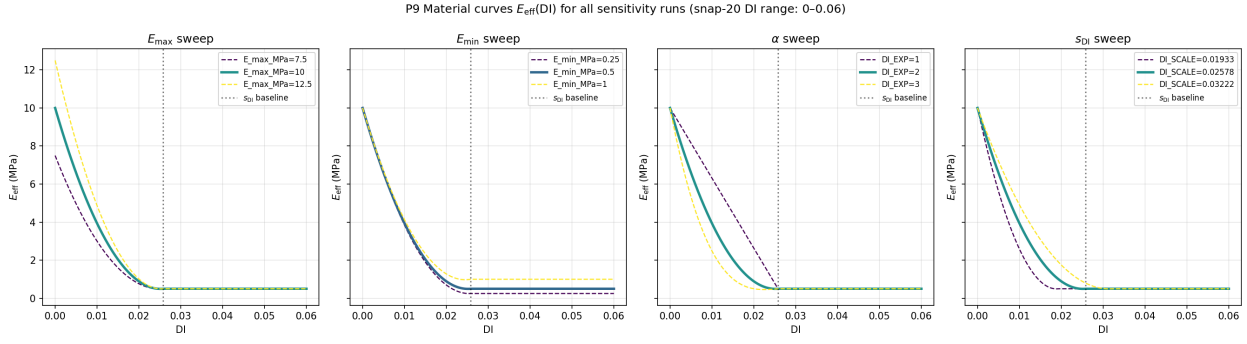


Figure 28: SensFig 4: $E_{\text{eff}}(\text{DI})$ model curves for all 12 parameter combinations. Solid line = baseline; dashed = variations. The snap-20 DI range (0–0.06) is indicated by the dashed vertical line. At late time ($\text{DI} \sim 0.5$ for DH-baseline), the model saturates at E_{min} regardless of E_{max} , α , or s_{DI} .

14 BC sensitivity: force vs displacement control (P10)

The current model applies a fixed inward pressure (force-controlled BC via *Cload). Under force control, the stress field is geometry-and-load dominated:

$$\sigma = F/A = \text{const} \quad \Rightarrow \quad u = \frac{\sigma L}{E_{\text{eff}}} \propto \frac{1}{E_{\text{eff}}}. \quad (12)$$

Therefore MISES is identical across conditions, while displacement scales with $1/E_{\text{eff}}$. Under displacement-controlled BC (prescribed inward-normal $\delta = \text{const}$):

$$u = \delta = \text{const} \quad \Rightarrow \quad \sigma = E_{\text{eff}} \frac{\delta}{L} \propto E_{\text{eff}}. \quad (13)$$

Now MISES scales with E_{eff} , while displacement is prescribed and identical.

Script p10_bc_sensitivity.py generated displacement-controlled INPs for DH-baseline and Commensal-static (late-time DI fields, $\delta = 1 \mu\text{m}$ inward-normal displacement on 6 228 free OUTER nodes; 2 892 Tie-slave APPROX nodes excluded).

BC type	Condition	MISES median (MPa)	$ U $ median (μm)
Force-ctrl ($C_{\text{load}} = 1 \text{ MPa}$)	DH-baseline	≈ 0.546	0.358
	Commensal-static	≈ 0.546	0.018
Disp-ctrl ($\delta = 1 \mu\text{m}$)	DH-baseline	0.669	0.270
	Commensal-static	13.19	0.270

The MISES ratio under displacement control is $13.19/0.669 \approx 19.7$, consistent with the E_{eff} ratio $9.85/0.50 \text{ MPa}$ (commensal vs. DH-baseline).

Key point. Key P10 findings:

Under force-controlled BC: displacement is the biomarker ($\times 19.7$); MISES is identical across conditions. Under displacement-controlled BC: MISES is the biomarker ($\times 19.7$, reversed); displacement is prescribed (same by definition). Both BCs confirm the same $\approx 19.7\times$ mechanical contrast, derived from the late-time E_{eff} ratio $9.85/0.50 \text{ MPa}$. The choice of BC determines which quantity carries the biological signal.

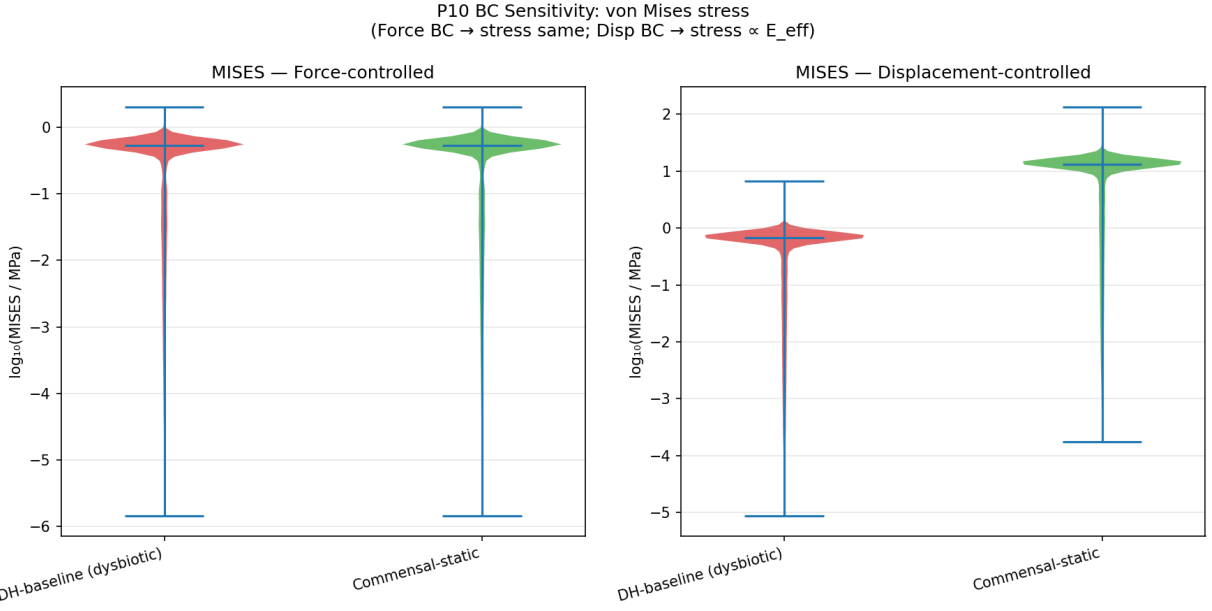


Figure 29: BCFig 1: Von Mises stress violin plots under force-ctrl (left) and displacement-ctrl (right) for DH-baseline and Commensal-static. Under force ctrl distributions overlap; under disp ctrl Commensal-static has $\approx 19.7\times$ higher MISES.

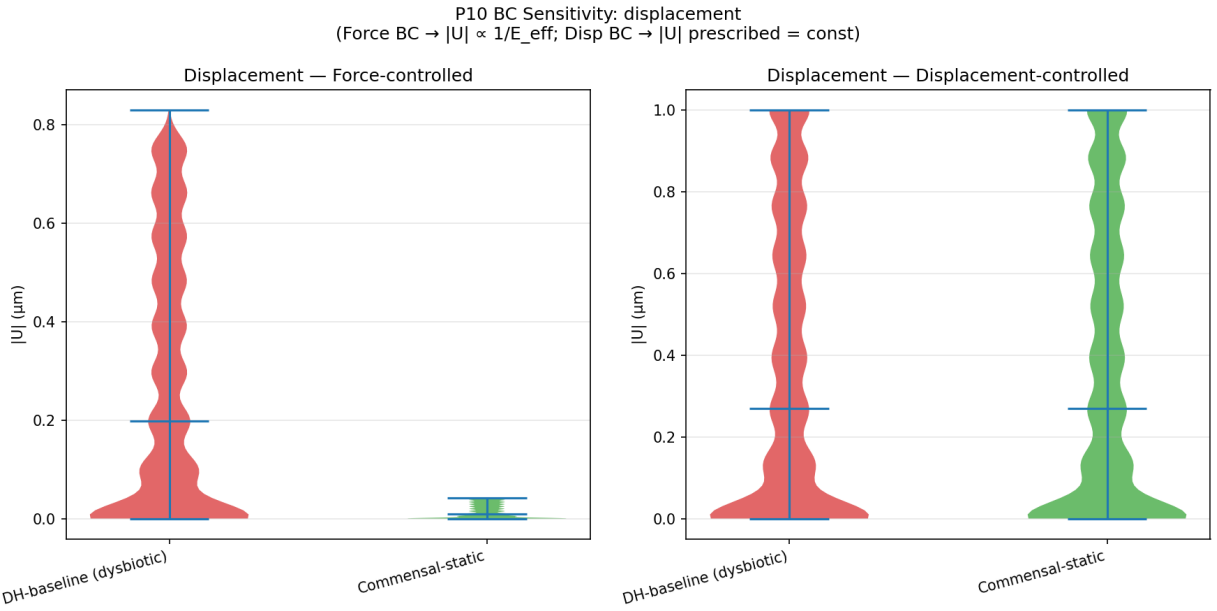


Figure 30: BCFig 2: Nodal displacement violin plots. Under force ctrl DH-baseline displacement is $\approx 19.7\times$ larger; under disp ctrl both conditions show the same prescribed value ($\delta = 1 \mu\text{m}$).

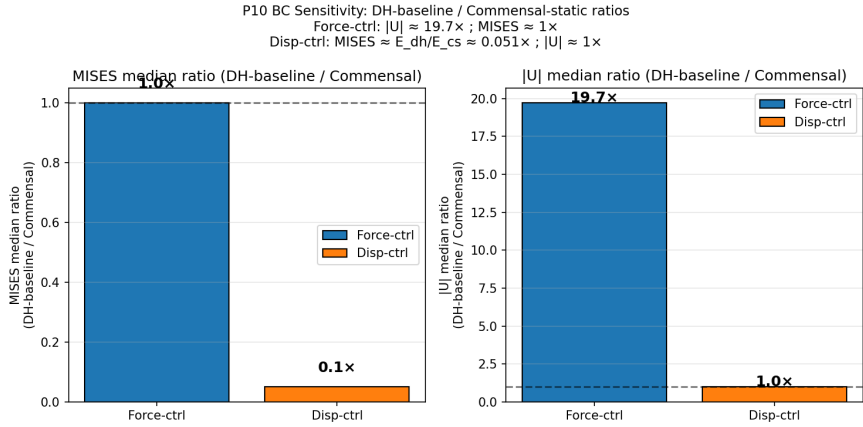


Figure 31: BCFig 3: Summary ratio bars (DH-baseline / Commensal-static) for MISES (left) and $|U|$ (right) under each BC type. The $\approx 19.7 \times$ contrast appears in displacement under force ctrl and in stress under displacement ctrl.

15 Documentation Roadmap

Document	Content	Status
FEM_PLAN.md	Pipeline status, next actions	✓ Done
biofilm_3tooth_report.tex (this file)	Full pipeline report + equations + P0 results	✓ Done
tmcmc_to_fem_coupling.py	P2 coupling script (DI field export + INP regen)	✓ Done
compare_conditions_fem.py	P0/P7 condition comparison: CompFig1–4	✓ Done
FEM_METHODS.md	Meshing algorithm, material model deep-dive	Medium
FEM_RESULTS.md	Tabulated MISES/U per run, parameter log	Planned
Jupyter fem_postprocess.ipynb	Interactive CSV exploration	Planned

A Material Bin Table

Material bins active in the current run (DI field from `abaqus_field_dh_3d.csv`, $t = 0.05$, snapshot 20):

Bin	$r = DI/s_{DI}$	E_{eff} (MPa)
3	0.300	$10(0.7)^2 + 0.5 \cdot 0.3 = 5.05$
4	0.375	$10(0.625)^2 + 0.5 \cdot 0.375 = 4.10$
5	0.450	$10(0.55)^2 + 0.5 \cdot 0.45 = 3.25$
6	0.525	$10(0.475)^2 + 0.5 \cdot 0.525 = 2.52$
7	0.600	$10(0.40)^2 + 0.5 \cdot 0.60 = 1.90$
8	0.675	$10(0.325)^2 + 0.5 \cdot 0.675 = 1.39$
9	0.750	$10(0.25)^2 + 0.5 \cdot 0.75 = 1.00$
10	0.825	$10(0.175)^2 + 0.5 \cdot 0.825 = 0.72$
11	0.900	$10(0.10)^2 + 0.5 \cdot 0.90 = 0.55$

Bins 0–2, 12–19 unused (outside DI field range for snapshot 20).

B ODB Extraction Details

`odb_extract.py` runs under ABAQUS Python (not standard Python). Key steps:

1. Open ODB read-only; retrieve the single instance.
2. Read node coordinates and element connectivity.

3. Compute element centroids via numpy vectorised mean of the 4 corner nodes.
4. Parse element sets T23/T30/T31_BIN_XX for tooth and bin membership.
5. Parse node sets T{23|30|31}_{INNER|OUTER|APPROX} in priority order (INNER < OUTER < APPROX) so APPROX overwrites OUTER for slit nodes.
6. Extract field outputs from the last frame of step LOAD: **U** (nodal), MISES (element, averaged over integration points).
7. Write `odb_nodes.csv` and `odb_elements.csv`.